CASE FILE
COPY

NACA TN No. 1648

NATIONAL ADVISORY COMMITTEE FOR AERONAUTICS

TECHNICAL NOTE

No. 1648

TANK TESTS OF A $\frac{1}{10}$-SIZE MODEL OF A HYPOTHETICAL FLYING BOAT WITH A HULL LENGTH-BEAM RATIO OF 9.0

By Marvin I. Haar

Langley Memorial Aeronautical Laboratory
Langley Field, Va.

Washington
July 1948

NATIONAL ADVISORY COMMITTEE FOR AERONAUTICS

TECHNICAL NOTE NO. 1648

TANK TESTS OF A $\frac{1}{10}$-SIZE MODEL OF A HYPOTHETICAL FLYING BOAT WITH A HULL LENGTH-BEAM RATIO OF 9.0

By Marvin I. Haar

SUMMARY

As part of a general investigation of the length-beam ratio of flying-boat hulls, the hydrodynamic characteristics of a powered dynamic model of a hypothetical flying boat with a hull length-beam ratio of 9.0 were investigated in Langley tank no. 1. This hull was one of a series also investigated in the Langley 300 MPH 7- by 10-foot tunnel to determine the aerodynamic effects of increasing the length-beam ratio.

The results indicated that increasing the hull length-beam ratio from 6 to 9 while holding the length^2-beam product constant introduces no serious adverse hydrodynamic characteristics attributable solely to the higher length-beam ratio. The effects of gross load, depth of step, angle of afterbody keel, and length of afterbody on the characteristics are shown to be approximately the same for the higher length-beam ratio as for conventional length-beam ratios. The use of a higher ratio to reduce aerodynamic drag therefore appears practicable hydrodynamically.

Relatively longer afterbodies may be desirable for higher length-beam-ratio hulls in order to obtain more satisfactory hydrodynamic longitudinal stability.

INTRODUCTION

In selecting the over-all proportions for a flying-boat hull, the effect of length-beam ratio (L/b) on the aerodynamic and the hydrodynamic characteristics is of primary importance and has been the subject of a number of tank and wind-tunnel investigations. The length is defined as the distance from the forward perpendicular (F.P.) to the stern-post (S.P.). The more significant information on the effect of length-beam ratio is contained in references 1 to 6.

One series of hulls tested in the Langley tanks attempted to eliminate the effect of size by maintaining a constant length-beam product, the height of the hull being assumed constant for all the models. An increase in length-beam ratio by this procedure reduced

the water resistance for a given load and improved the spray characteristics (reference 1). No information was obtained on the hydrodynamic stability characteristics. Appreciable differences in aerodynamic drag with change in length–beam ratio would not be expected for this series of hulls.

A further analysis of the resistance characteristics (reference 2) and of spray characteristics of a number of full–size flying boats (reference 5) indicated that if the length–beam ratio were increased, the length^2–beam product being maintained constant, the size of the hull and, consequently, the aerodynamic drag might be reduced with no significant changes in hydrodynamic resistance or spray characteristics.

In order to determine the actual reduction in aerodynamic drag with increase in length–beam ratio with a constant length^2–beam product, a series of hulls was designed which had the same length^2–beam product as a Navy twin–engine flying boat. This seaplane, which has a length–beam ratio of 6.3, was known to have good hydrodynamic characteristics, and it was considered desirable to maintain these characteristics and to realize possible advantages of the high length–beam ratio in terms of reductions in aerodynamic drag of the hull. The aerodynamic drag of this series was determined in the Langley 300 MPH 7– by 10–foot tunnel. The results (reference 6), which included the interference of a thick wing, indicate that a reduction in hull drag of approximately 30 percent is realized by an increase in length–beam ratio (constant length^2–beam product) from 6 to 15.

As a preliminary hydrodynamic investigation of this same series of hulls, the hydrodynamic stability, resistance, and spray characteristics were determined for the model having a basic hull length–beam ratio of 9.0. Several modifications (change in depth of step, angle of afterbody keel, and length of afterbody) were tested to determine whether the hydrodynamic trends with hull variations would be the same for a length–beam ratio of 9.0 as were previously found for lower length–beam ratios (approx. 6). The spray characteristics for this model have been described in reference 7.

DESCRIPTION OF MODEL

The model used for the investigation, Langley tank model 203A, was a $\frac{1}{10}$-size powered dynamic model of a hypothetical flying boat generally similar to a Navy twin–engine seaplane, which has a length–beam ratio of 6.3. The length and beam of the hull were derived by increasing the length of the forebody and afterbody and decreasing the beam in such a manner that the length^2–beam product was maintained the same as for the Navy seaplane. The form, size, and relative location of the aerodynamic surfaces of model 203A corresponded to those of the

Navy seaplane. A more detailed discussion of the derivation of the hull with a length–beam ratio of 9.0 is given in references 6 and 7.

Photographs of model 203A, lines of the hull, and the general arrangement are shown in figures 1, 2, and 3, respectively. The general arrangements of the length–beam model and the Navy seaplane model are compared in figure 3, and a further comparison of the dimensions of model 203A with corresponding dimensions of a model of the Navy seaplane is given in table I. The increase in length–beam ratio from 6.3 to 9.0, on the basis of a constant length^2–beam product and small changes in fairing, produced the following reductions in hull dimensions: maximum frontal area, 23 percent; volume, 11 percent; and skin area, 4 percent.

Ten modifications of the basic hull were tested. The formation of typical modifications is shown in figure 4. Changes in afterbody length necessarily caused some variation from the basic length–beam ratio of 9.0 inasmuch as a constant forebody length and beam were maintained. The following table lists the model designation and description of the various configurations in the sequence in which they were tested:

Model	Length of afterbody		Depth of step		Angle of afterbody keel (deg)	Sternpost angle (deg)
	Inches	Beams	Inches	Percent beam		
203A	37.64	3.8	0.89	9.0	5.4	6.7
203A–1	37.64	3.8	1.28	13.0	5.4	7.3
203B	29.16	3.0	.89	9.0	5.4	7.1
203B–1	29.16	3.0	1.28	13.0	5.4	7.9
203A–1–a	37.64	3.8	1.28	13.0	7.4	9.3
203A–2–a	37.64	3.8	1.65	17.0	7.4	9.8
203A–3	37.64	3.8	.49	5.0	5.4	6.1
203A–b	37.64	3.8	.89	9.0	3.5	4.9
203C	46.14	4.7	.89	9.0	5.4	6.5
203C–1	46.14	4.7	1.28	13.0	5.4	6.9

The model was powered by two $1\frac{1}{4}$-horsepower variable–frequency motors each driving a three–blade propeller. Slats were attached to the leading edge of the wing to delay the stall to an angle more nearly equal to that expected for the full–size airplane. The pitching moment of inertia of the ballasted model at a gross weight of 52.0 pounds was 6.8 slug–feet^2.

APPARATUS AND PROCEDURE

The towing equipment of Langley tank no. 1 is described in reference 8. A description of some of the test procedures used for this investigation is presented in references 7 and 9.

The effective thrust was determined by towing the model in the air at zero flap deflection and zero trim with the step located 8 inches above the surface of the water. The horizontal force with the propellers removed and with the propellers turning was measured. With a blade angle of 14° at 0.75 radius and a rotational speed of 4550 rpm, the effective thrust (fig. 5) was approximately equal to the scale thrust of the Navy seaplane.

When the aerodynamic lift and pitching moments were determined, the center of moments was located at 24 percent mean aerodynamic chord and the flaps were deflected 20°. With power, aerodynamic tests were made over a range of speed from 0 to 40 feet per second for three deflections of the elevator, 0°, −10°, and −20°. Without power, the aerodynamic lift and pitching moments were measured at a speed of 40 feet per second for an elevator deflection of −10°. The usual NACA aerodynamic lift and pitching-moment coefficients were computed from these data for a carriage speed of 40 feet per second. The results of the aerodynamic tests are presented in figures 6 and 7.

The hydrodynamic investigation was made with flaps deflected 20° and at gross loads corresponding to those of the Navy seaplane. Inasmuch as the beam of the model was smaller than that of conventional designs, the gross load coefficient of model 203A was substantially higher than that associated with existing conventional flying-boat hulls. Gross load coefficient C_{Δ_o} is defined as follows:

$$C_{\Delta_o} = \frac{\Delta_o}{wb^3}$$

where

Δ_o gross load, pounds

w specific weight of water, pounds per cubic foot (63.5 lb/cu ft for these tests)

b maximum beam, feet

The gross loads and the corresponding gross load coefficients for hulls having length–beam ratios of 6.3 and 9.0 are given in the following table:

Gross load (lb)		Gross load coefficient, C_{Δ_o}	
Full size	$\frac{1}{10}$-size model	Model 203A, $\frac{L}{b} = 9$	Navy seaplane, $\frac{L}{b} = 6.3$
62,000	61.5	1.77	0.87
65,000	64.5	1.85	.90
72,000	71.5	2.05	1.00
82,000	81.5	2.34	1.14
92,000	91.5	2.62	1.28

The trim limits of stability were determined with full power at constant speeds for gross loads of 61.5 and 81.5 pounds. The range of stable position of the center of gravity was determined by making take–offs with full power at an acceleration of 1 foot per second per second. Take–off runs were made at various positions of the center of gravity for three deflections of the elevator, 0°, −10°, and −20°, and at gross loads of 61.5 and 81.5 pounds. Take–offs of model 203A were made at a gross load of 64.5 pounds.

The landing stability was investigated at various trims by flying the model with one–quarter static thrust at the desired trim and then decelerating the towing carriage at a uniform rate of 2 feet per second per second. Landings were usually made at two positions of the center of gravity, 28 percent and 36 percent mean aerodynamic chord, and at two gross loads, 61.5 pounds and 81.5 pounds. Records of the change in trim and draft were obtained to show the behavior of the models during landings. Zero draft was taken as the vertical position at which the main step touched the water at zero trim.

The resistance of the complete model was measured with the center of gravity at 28 percent mean aerodynamic chord, an elevator deflection of −10°, and zero power. The resistance was determined at gross loads ranging from 61.5 to 81.5 pounds.

The spray characteristics of the model were evaluated by observing the spray and taking photographs at constant and accelerated speeds for gross loads from 65.0 to 91.5 pounds. These tests were made with full power, the center of gravity at 28 percent mean aerodynamic chord, and the elevators deflected −10°.

Trim is defined as the included angle between the forebody keel at the step and the water surface. Moments tending to raise the bow are considered positive.

RESULTS

Representative hydrodynamic data for each configuration are presented in figures 8 to 17. The following data are included wherever available:

(a) Trim limits of stability with full power
(b) Variation of trim and total resistance with speed, power off
(c) Records showing the variation of trim and draft during landing
(d) Variation in trim with speed during take-off for various deflections of the elevator and positions of the center of gravity
(e) Maximum amplitude of porpoising during take-off at several positions of the center of gravity

On those modifications where the lower trim limit of stability was not determined, the lower limit of model 203A is shown with a dashed line. Test points have been omitted for all the trim tracks except those of model 203A.

The effects of the various hull parameters on trim limits of stability, maximum amplitude of porpoising at different positions of the center of gravity, and total resistance are shown in figures 18, 19, and 20, respectively. Bow and stern spray photographs of model 203C-1 are presented as figures 21 and 22. The range of speed over which spray entered the propellers is shown in figure 23.

DISCUSSION

A study of the results presented in reference 7 and figure 9 of the present paper shows no adverse spray, stability, or resistance effects that would prevent operation of a full-size flying boat having a length-beam ratio of 9.0. At the design gross load of 61.5 pounds satisfactory take-offs (maximum amplitude of porpoising of 2°) could be made over a range of position of the center of gravity of approximately 10 percent mean aerodynamic chord at a fixed elevator deflection of -10°. Model 203A-1 did not skip at any contact trim investigated. At contact trims above 10° there was a slight tendency towards upper-limit porpoising. The resistance of model 203A-1 compared favorably with the resistance curves of models having conventional length-beam ratios in the neighborhood of 5 or 6. An increase in the length of afterbody from 3.8 to 4.7 beams (giving an over-all length-beam ratio of 9.9), model 203C-1, effected an improvement in the longitudinal take-off stability. The long afterbody of model 203C-1 limited upper-limit porpoising to approximately $2\frac{1}{2}$°. Take-offs with

a fixed elevator deflection of -10° could therefore be made at any practicable after position of the center of gravity without exceeding $2\frac{1}{2}^{\circ}$ amplitude of porpoising.

The effects of such hull variables as length of afterbody, depth of main step, angle of afterbody keel, and gross load upon the trim limits of stability, range of position of the center of gravity for stable take-off, landing stability, and resistance of flying-boat hulls of contemporary design are presented in references 10 to 14. In discussing the results of the present tests, the various hull modifications are presented in relation to their effect on the principal hydrodynamic characteristics.

Trim Limits of Stability

The trim limits of stability were generally similar to those obtained for models with conventional length-beam ratios. The effect of changes in the afterbody configuration is shown in figure 18. Changes in length of afterbody, depth of step, or angle of afterbody keel had no effect on the lower trim limit of stability except at low speeds near the hump. Modifications that increased the sternpost angle generally raised the hump of the lower limit. An increase in angle of afterbody keel, decrease in afterbody length, or increase in depth of step all raised the upper trim limits. An increase in gross load raised all the trim limits to higher trims. These trends are similar to those obtained for conventional length-beam ratios (references 10 to 12).

For most modifications, the model could be made to porpoise over a small range of intermediate planing speeds so that the upper and lower trim limits were exceeded at the extreme ends of the trim cycle. If the amplitude of porpoising was allowed to build up to exceed both the upper and lower limits, stability could not be recovered by means of the elevators alone. Although this characteristic is undesirable, the maneuver required to obtain this porpoising between the upper and lower trim limits was abnormal. Tests of several models of conventional length-beam ratios have shown similar "porpoising between limits," which was not revealed in full-size tests. In normal seaplane operations, it is often possible to accelerate through an unstable range before the amplitude of porpoising has a chance to build up to violent proportions; whereas, in the tank investigation, the trim limits are determined at constant speed, and the porpoising amplitude is allowed to build up to a maximum. An increase in length-beam ratio on the basis of a constant length^2-beam product is believed, however, to aggravate the porpoising between limits.

Of the parameters investigated, the length of afterbody had the most pronounced effect on the trim limits of stability (fig. 18). Increasing the length of afterbody to 4.7 beams eliminated the porpoising

between limits. With the long afterbody the maximum amplitude of porpoising was apparently reduced to such an extent that the extreme ends of the porpoising cycle could not exceed both of the trim limits. Increasing the angle of afterbody keel or depth of step reduced the range of speed over which this erratic porpoising occurred. This reduction might be expected inasmuch as the upper trim limits were raised by these modifications, and the range of speeds over which porpoising could exceed both of the limits on the same cycle was therefore reduced.

Center-of-Gravity Limits for Stable Take-Off

The variation in trim with speed for take-off at various positions of the center of gravity and with various deflections of the elevators was obtained for four of the modifications (203A, 203A-1, 203B, and 203C-1). The summary plots of the maximum amplitude of porpoising were made from these trim tracks.

Changes in the depth of step and length of afterbody (fig. 19) or gross load (figs. 9, 10, and 17) had no pronounced effect on the range of position of the center of gravity for stable take-off. This result is in agreement with results obtained for models having conventional length-beam ratios (references 10 and 12). As the length of afterbody was increased, however, the slope of the after-limit curves tended to decrease; the after-limit curves became flatter and the maximum amplitudes of porpoising at after positions of the center of gravity were reduced (fig. 19).

Landing Stability

There was no violent skipping on any modification tested. Landings at contact trims above the upper trim limit, increasing trim, generally resulted in some upper-limit porpoising during the landing runout. The effects of the various parameters on the landing stability were approximately the same as for models having conventional length-beam ratios (references 10 to 12). There were no adverse effects on the landing stability as a result of increasing the length-beam ratio.

Increasing the depth of the main step generally improved the landing stability, with respect to both skipping and porpoising. (Compare landing charts for model 203A-1-a having a depth of step of 13 percent beam and model 203A-2-a having a depth of step of 17 percent beam, figs. 12 and 13, respectively; compare landing charts for model 203C having a depth of step of 9 percent beam and model 203C-1 having a depth of step of 13 percent beam, figs. 16 and 17, respectively.) With a constant depth of step, landings appeared to be slightly more unstable, especially with the heavy load, as the length of afterbody was increased. (Compare landing charts for model 203B-1 having an afterbody length of 3.0 beams, model 203A-1 having an afterbody length

of 3.8 beams, and model 203C–1 having an afterbody length of 4.7 beams, figs. 11, 9, and 17, respectively.)

An increase in the angle of afterbody keel from 5.4° to 7.4° (models 203A–1 and 203A–1–a) gave slightly worse landing stability (figs. 9 and 12). Model 203A–1 did not skip when landing, but model 203A–1–a usually tended to skip at landing trims above 6°, especially at the heavy load. A decrease in the angle of afterbody keel from 5.4° to 3.5° (models 203A, no landing charts, and 203A–b, fig. 15) also resulted in less landing stability. These results are consistent with those obtained for hulls of lower length–beam ratio. At the higher landing trims, with model 203A–b upper–limit porpoising of fairly large amplitude was encountered on contact with the water.

Increasing the gross load from 61.5 to 81.5 pounds generally had no appreciable effect on the landing stability of all configurations.

Resistance

The effects of depth of step, angle of afterbody keel, and gross load on the resistance and trim were the same as for models with conventional length–beam ratios (references 13 and 14). Modifications that decreased the sternpost angle generally decreased the resistance and trim at hump speed, increased the resistance at high speeds, and shifted the hump resistance to higher speeds (fig. 20). The data presented in figure 20 are for a gross load of 64.5 pounds.

Increasing the gross load increased the resistance and trim over the entire speed range of all configurations.

Spray Characteristics

In reference 7, the over–all spray characteristics of model 203A were adjudged acceptable up to an initial gross load of 81.5 pounds (gross load coefficient of 2.3). Bow and stern spray photographs comparable with those shown for model 203A in reference 7 were obtained for model 203C–1 and are presented as figures 21 and 22. There was no substantial difference in the spray characteristics of the two configurations. The long afterbody of model 203C–1 produced lower trims and increased slightly the amount of spray entering the propellers. The range of speed over which the bow blister entered the propellers (fig. 23) was approximately the same for model 203C–1 as for model 203A. The range of speeds over which loose spray entered the propellers was shifted to slightly lower speeds.

The amount of spray striking the flaps with full power was not excessive and can be observed in figure 22. The range of speed over which spray struck the flaps for model 203C–1 was approximately the same as for model 203A.

CONCLUSIONS

The hydrodynamic characteristics of a powered dynamic model of a hypothetical flying boat with a hull length–beam ratio of 9.0 were investigated in Langley tank no. 1, and the following conclusions were indicated:

1. On the basis of a constant length^2–beam product and a given gross weight, the size of a flying-boat hull and, consequently, the aerodynamic drag can be reduced by increasing the length–beam ratio from 6 to 9 with no serious adverse hydrodynamic stability or resistance characteristics that can be attributed solely to the increased length–beam ratio of the hull.

2. The effect of such hull parameters as gross load, depth of step, angle of afterbody keel, and length of afterbody on the trim limits of stability, range of position of the center of gravity for stable take-off, landing stability, and power-off total resistance is approximately the same for a model with a length–beam ratio of 9 as for hulls with a length–beam ratio of 5 or 6.

3. It may be desirable at higher length–beam ratios to incorporate longer afterbodies than are indicated by the use of the criterion of a constant length^2–beam product in order to obtain more satisfactory longitudinal stability characteristics.

Langley Memorial Aeronautical Laboratory
National Advisory Committee for Aeronautics
Langley Field, Va., March 17, 1948

REFERENCES

1. Bell, Joe W., Garrison, Charlie C., and Zeck, Howard: Effect of Length–Beam Ratio on Resistance and Spray of Three Models of Flying–Boat Hulls. NACA ARR No. 3J23, 1943.

2. Land, Norman S., Bidwell, Jerold M., and Goldenbaum, David M.: The Resistance of Three Series of Flying–Boat Hulls as Affected by Length–Beam Ratio. NACA ARR No. L5G23, 1945.

3. Bidwell, Jerold M., and Goldenbaum, David M.: Resistance Tests of Models of Three Flying–Boat Hulls with a Length–Beam Ratio of 10.5. NACA ARR No. L5G19, 1945.

4. Davidson, Kenneth S. M., and Locke, F. W. S., Jr.: General Tank Tests on the Hydrodynamic Characteristics of Four Flying–Boat Hull Models of Differing Length–Beam Ratio. NACA ARR No. 4F15, 1944.

5. Parkinson, John B.: Design Criterions for the Dimensions of the Forebody of a Long–Range Flying Boat. NACA ARR No. 3K08, 1943.

6. Yates, Campbell C., and Riebe, John M.: Effect of Length–Beam Ratio on the Aerodynamic Characteristics of Flying–Boat Hulls. NACA TN No. 1305, 1947.

7. Olson, Roland E., and Bell, Joe W.: Spray Characteristics of a Powered Dynamic Model of a Flying Boat Having a Hull with a Length–Beam Ratio of 9.0. NACA ARR No. L5L29, 1946.

8. Truscott, Starr: The Enlarged N.A.C.A. Tank, and Some of Its Work. NACA TM No. 918, 1939.

9. Olson, Roland E., and Land, Norman S.: Methods Used in the NACA Tank for the Investigation of the Longitudinal–Stability Characteristics of Models of Flying Boats. NACA Rep. No. 753, 1943.

10. Truscott, Starr, and Olson, Roland E.: The Longitudinal Stability of Flying Boats as Determined by Tests of Models in the NACA Tank. II – Effect of Variations in Form of Hull on Longitudinal Stability. NACA ARR, Nov. 1942.

11. Land, Norman S., and Lina, Lindsay J.: Tests of a Dynamic Model in NACA Tank No. 1 to Determine the Effect of Length of Afterbody, Angle of Afterbody Keel, Gross Load, and a Pointed Step on Landing and Planing Stability. NACA ARR, March 1943.

12. Olson, Roland E., and Land, Norman S.: Effect of Afterbody Length and Keel Angle on Minimum Depth of Step for Landing Stability and on Take-Off Stability of a Flying Boat. NACA TN No. 1571, 1948.

13. Bell, Joe W., and Willis, John M., Jr.: The Effects of Angle of Dead Rise and Angle of Afterbody Keel on the Resistance of a Model of a Flying-Boat Hull. NACA ARR, Feb. 1943.

14. Bell, Joe W.: The Effect of Depth of Step on the Water Performance of a Flying-Boat Hull – NACA Model 11-C. NACA TN No. 535, 1935.

TABLE I

COMPARISON OF BASIC DIMENSIONS OF MODELS 203A AND NAVY SEAPLANE

	Model 203A	Navy seaplane model
Hull:		
Maximum beam, in.	9.85	12.50
Length:		
Forebody, bow to step, in.	51.04	45.30
Length–beam ratio	5.2	3.6
Afterbody, step to sternpost, in.	37.64	33.40
Length–beam ratio	3.8	2.7
Tail extension, sternpost to after perpendicular, in.	27.97	35.00
Over all, bow to after perpendicular, in.	116.65	113.70
Step:		
Type	Transverse	Transverse
Depth at keel, in.	0.89	1.10
Depth at keel, percent beam	9	9
Angle of forebody keel to base line, deg	0	0
Angle of afterbody keel to base line, deg	5.4	5.4
Angle of sternpost to base line, deg	6.7	7.2
Angle of dead rise of forebody		
Excluding chine flare, deg	20	20
Including chine flare, deg	15.9	17.9
Angle of dead rise of afterbody, deg	20	20
Wing:		
Area, sq ft	18.26	18.26
Span, ft	13.97	13.97
Root chord, in.	19.20	19.20
Angle of incidence, deg	4	4
Mean aerodynamic chord (M.A.C.)		
Length, projected, in.	16.48	16.48
Leading edge aft of bow, in.	43.04	37.30
Leading edge forward of step, in.	8.0	8.0
Leading edge above base line, in.	18.34	18.35
Horizontal tail surface:		
Area, sq ft	3.33	3.33
Span, ft	4.3	4.3
Angle of stabilizer to wing chord, deg	−4	−4
Elevator root chord, in.	3.84	3.84
Elevator semispan, ft	1.67	1.67
Length from 25 percent M.A.C. of wing to hinge line of elevators, in.	59.4	59.4
Height above base line, in.	22.80	22.80
Propellers:		
Number of propellers	2	2
Number of blades	3	3
Diameter, in.	19.8	19.8
Angle of thrust line to base line, deg	2	2
Angle of blade at 0.75 radius, deg	14	14
Clearance above keel line, in.	9.9	9.9

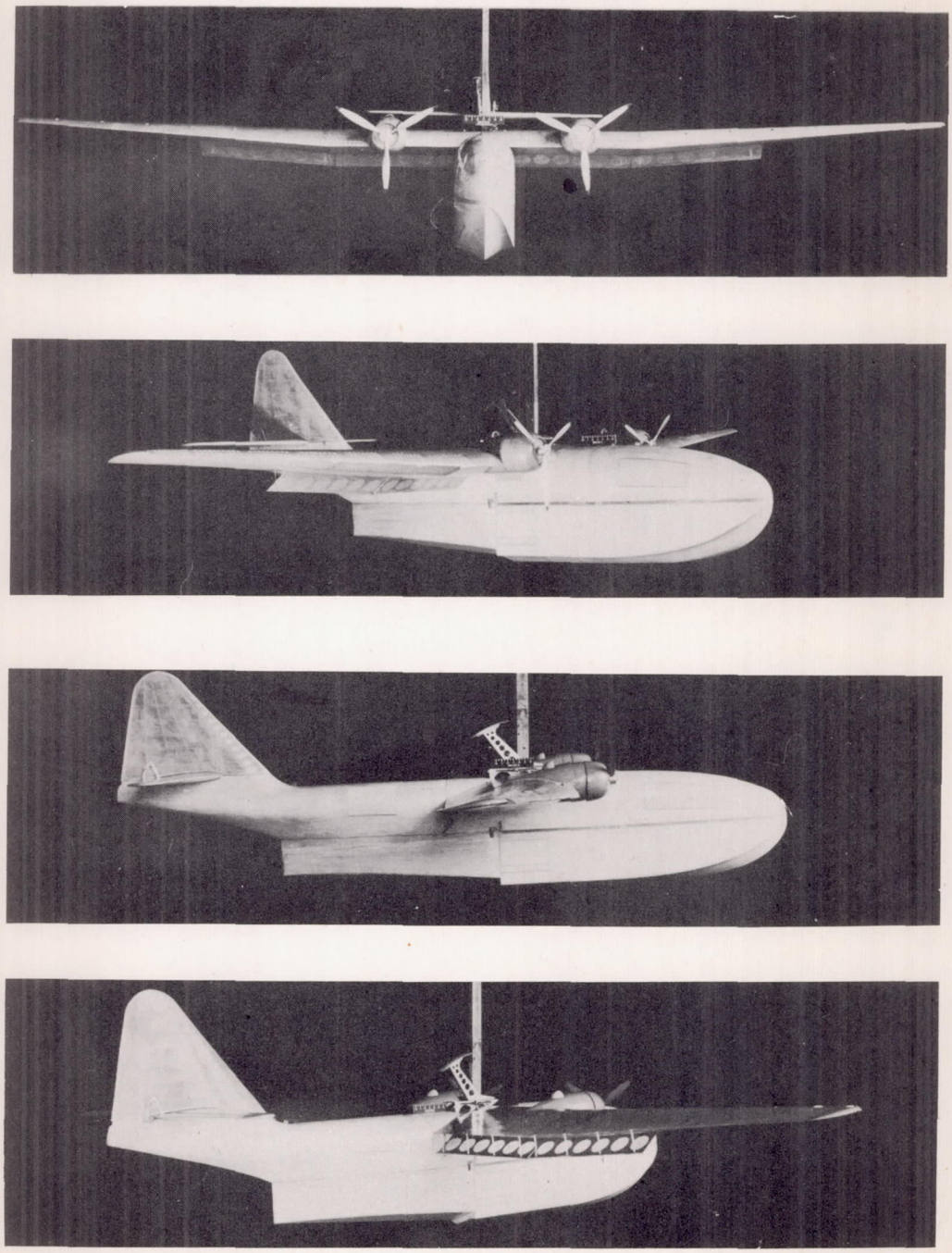


Figure 1.- Model 203A.

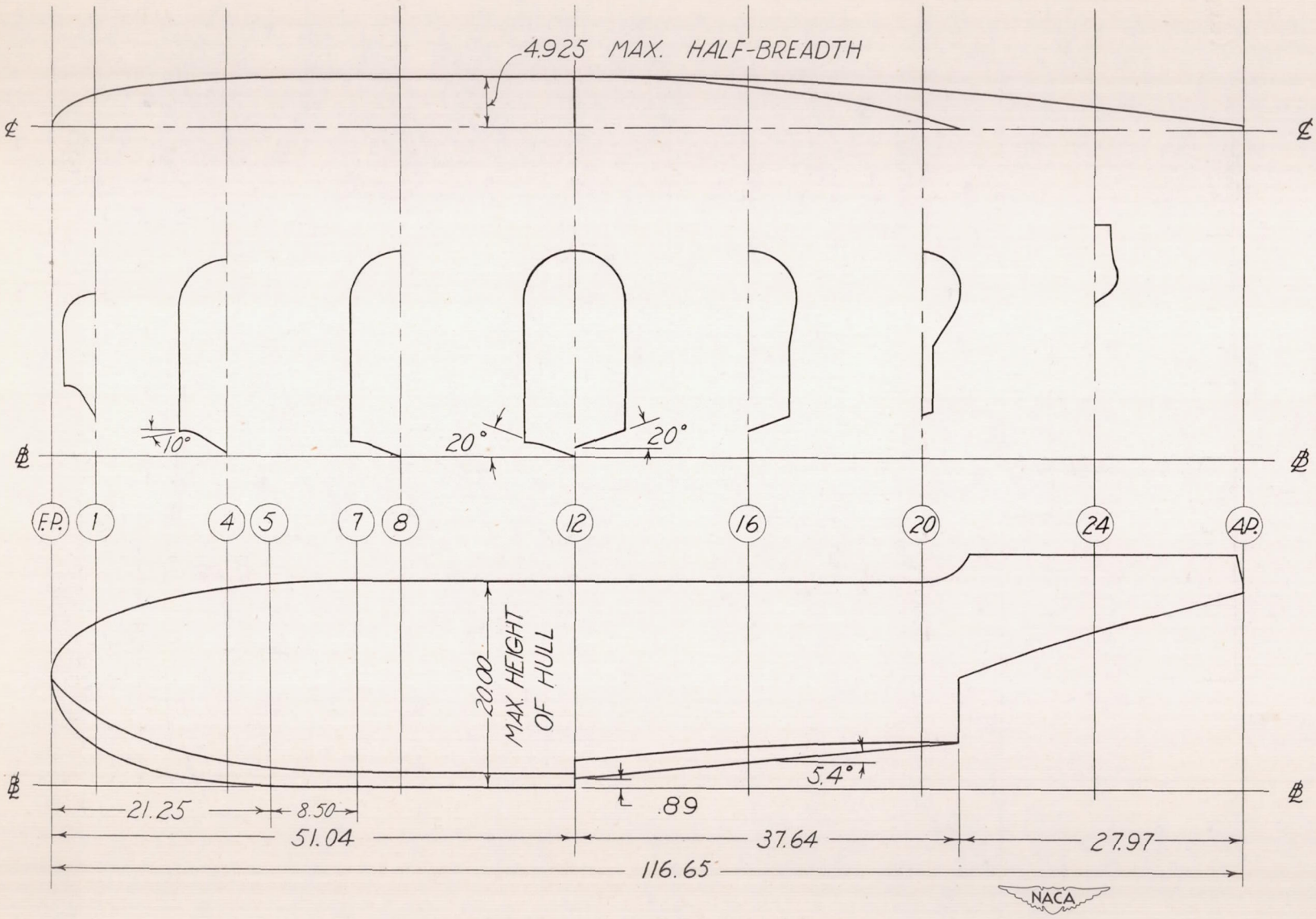


Figure 2.- Lines of hull of model 203A. (All dimensions are in inches.)

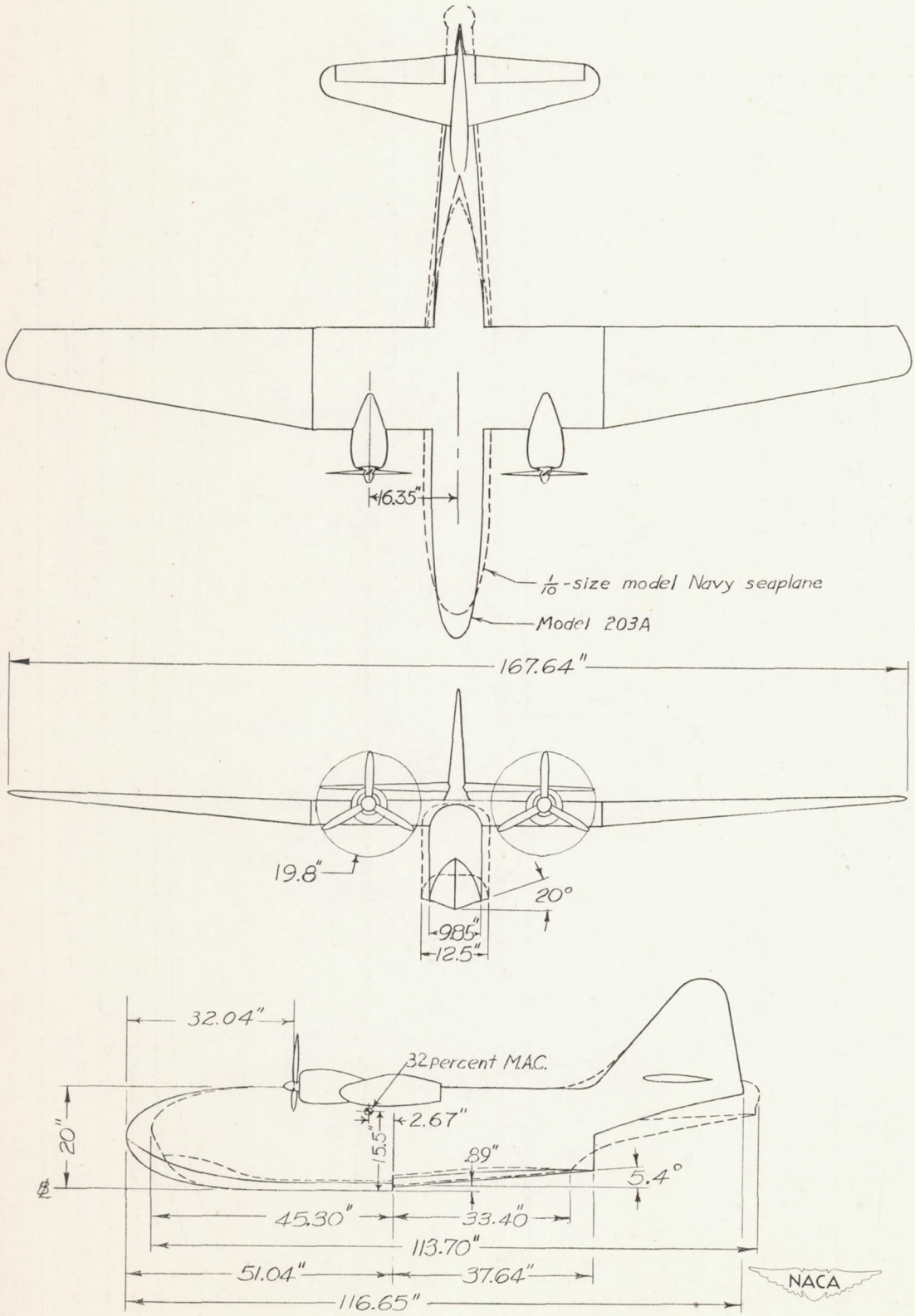
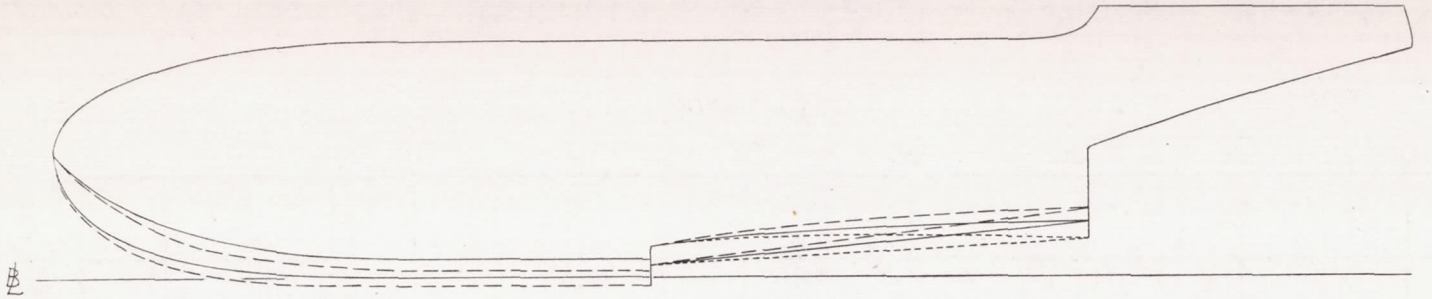


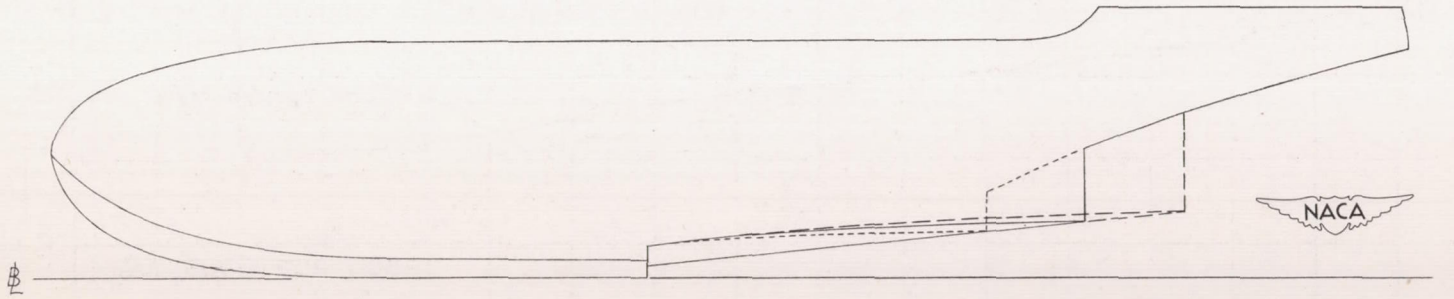
Figure 3.- Comparison of model 203A with $\frac{1}{10}$-size model Navy seaplane.

Model	Length of afterbody, in.	Depth of step, in.	Angle of after-body keel, deg
——— 203A	37.64	0.89	5.4
····· 203A-b	37.64	.89	3.5
– – – – 203A-2-a	37.64	1.65	7.4



(a) Depth of step and angle of afterbody keel.

——— 203A	37.64	0.89	5.4
····· 203B	29.16	.89	5.4
– – – – 203C	46.14	.89	5.4



(b) Length of afterbody.

Figure 4.- Typical modifications to model 203A.

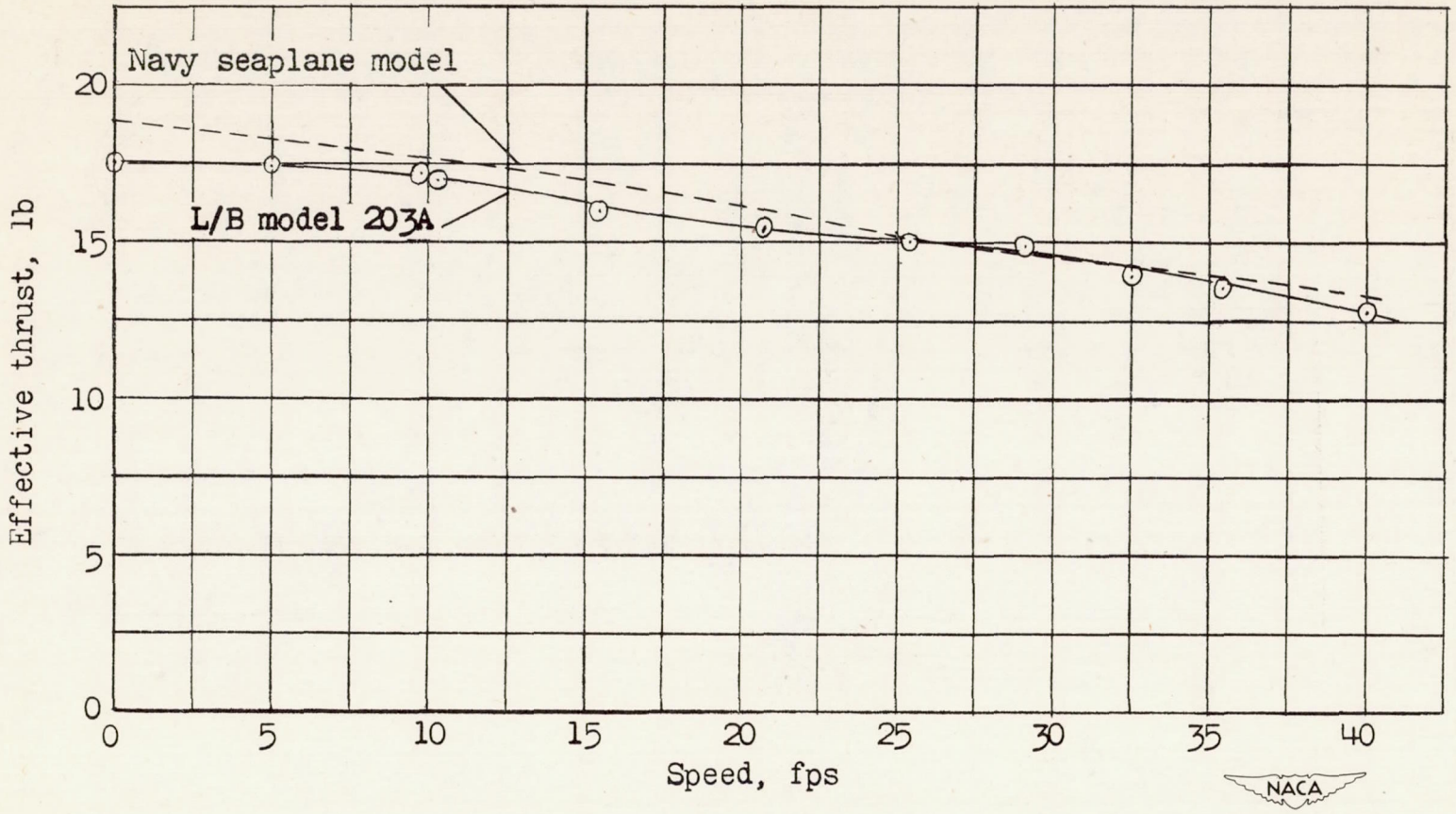
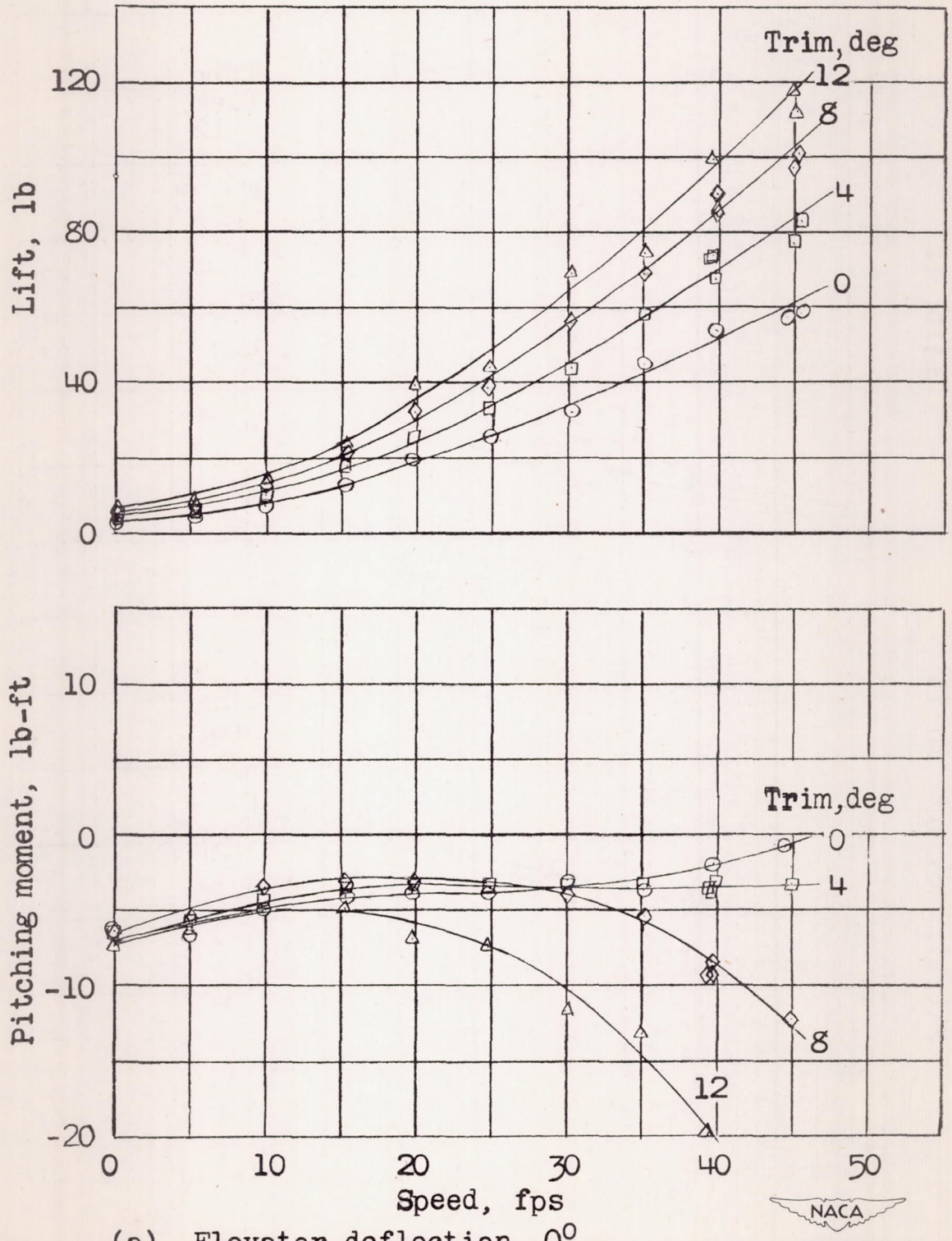
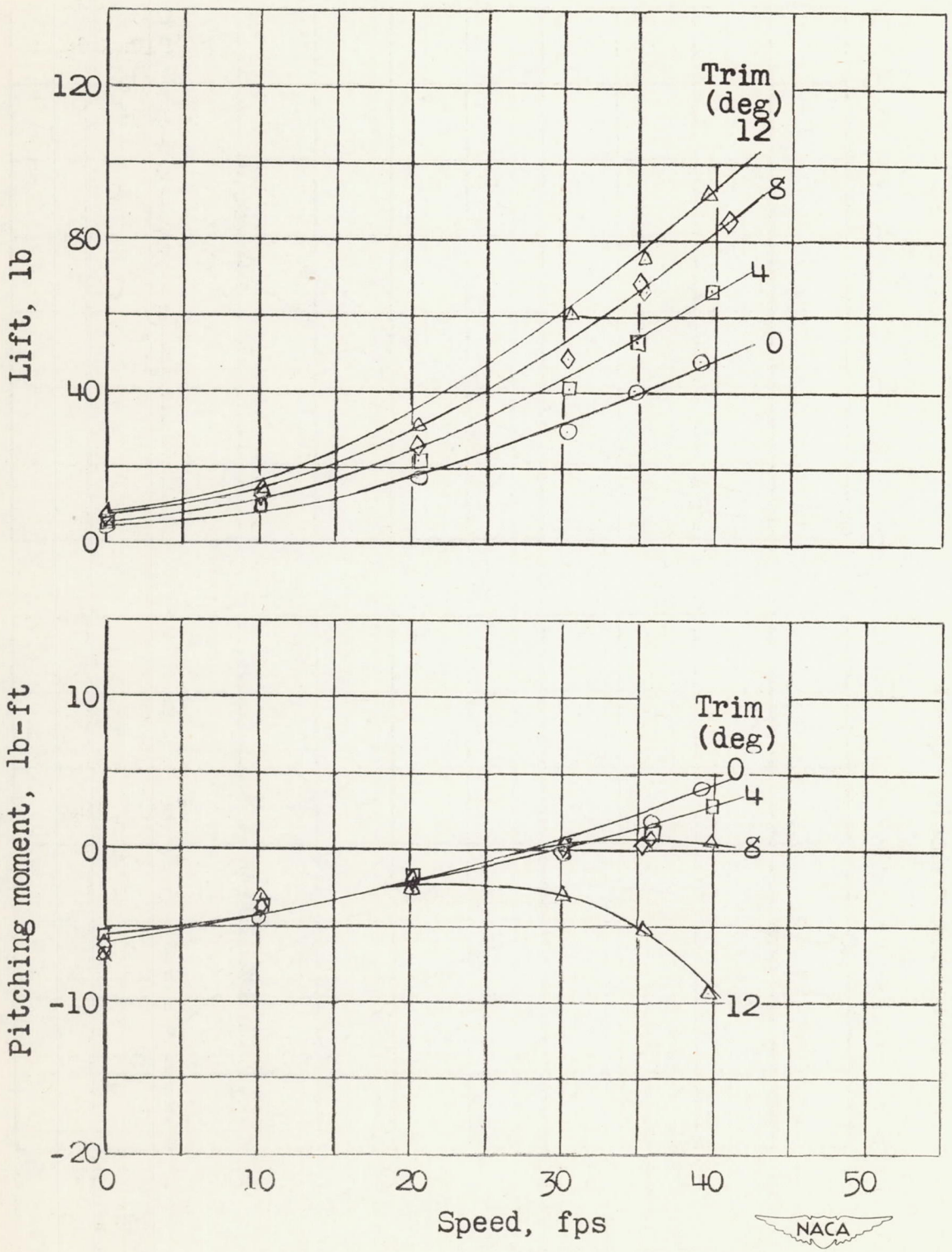


Figure 5.- Variation of effective thrust with speed. Full power, 4550 rpm; blade angle, 14°; flap deflection, 0°; trim, 0°; model 203A.



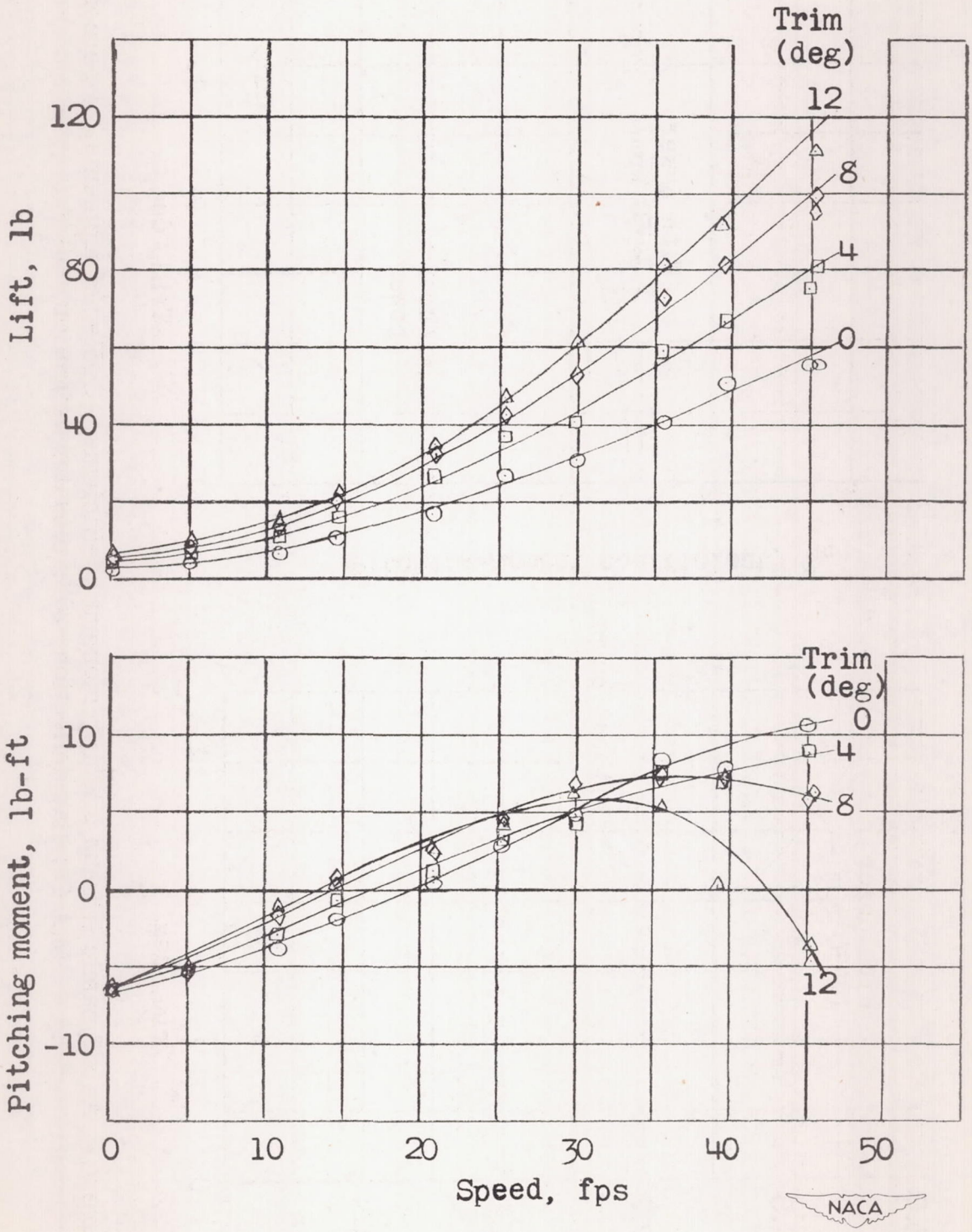
(a) Elevator deflection, 0°.

Figure 6.- Variation in aerodynamic lift and pitching moment with speed. Full power, 4550 rpm; center of moments, 24 percent M.A.C.; flap deflection, 20°.



(b) Elevator deflection, -10°.

Figure 6.- Continued.



(c) Elevator deflection, -20°.

Figure 6.- Concluded.

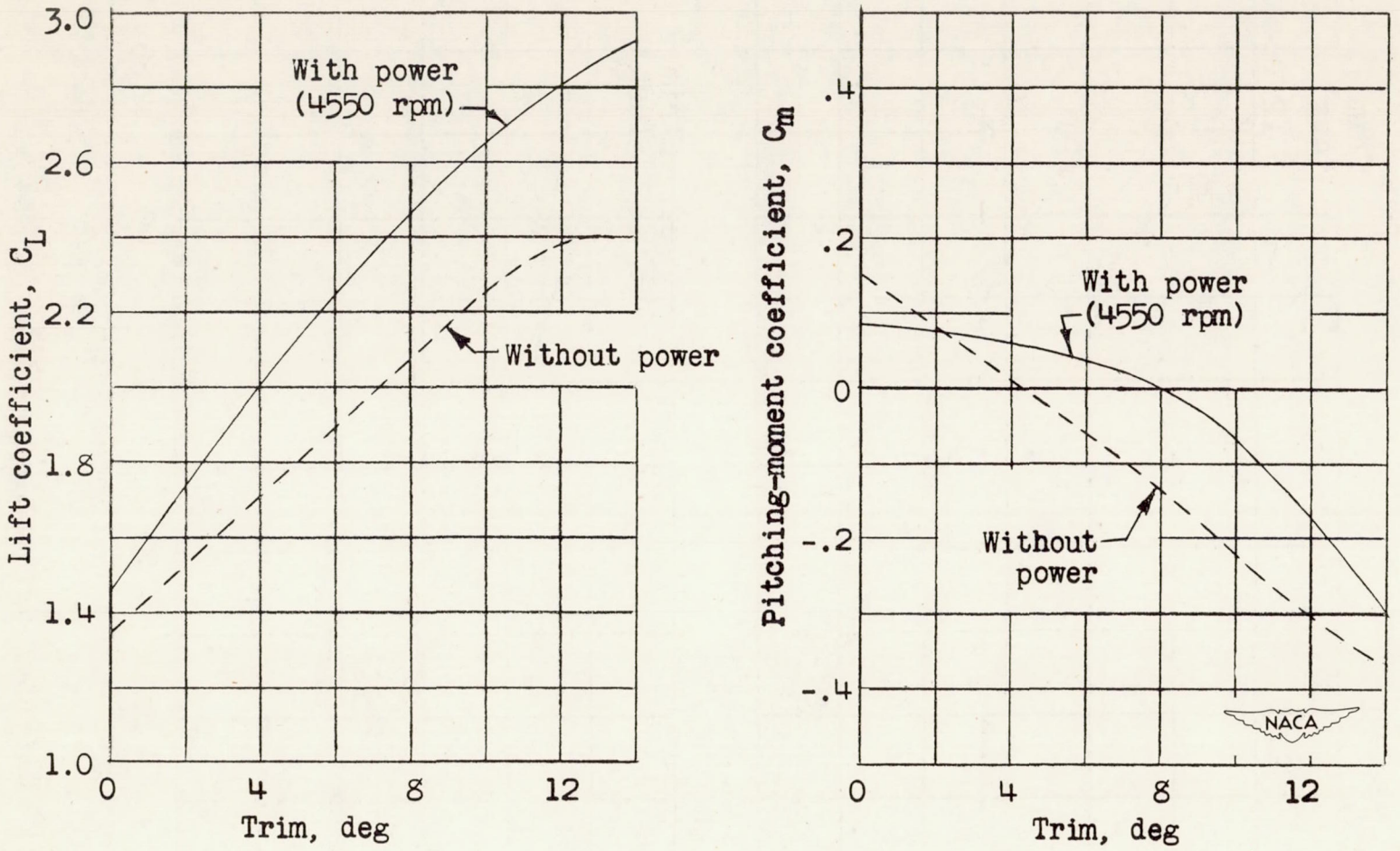
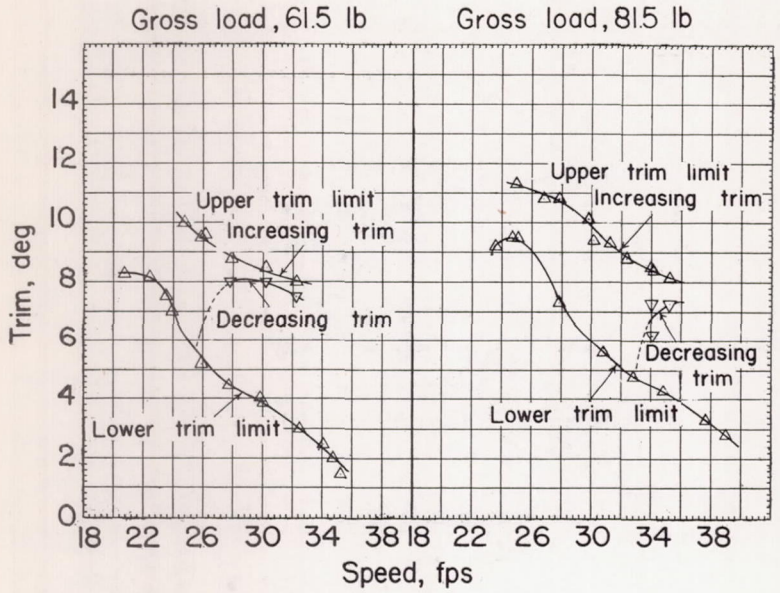
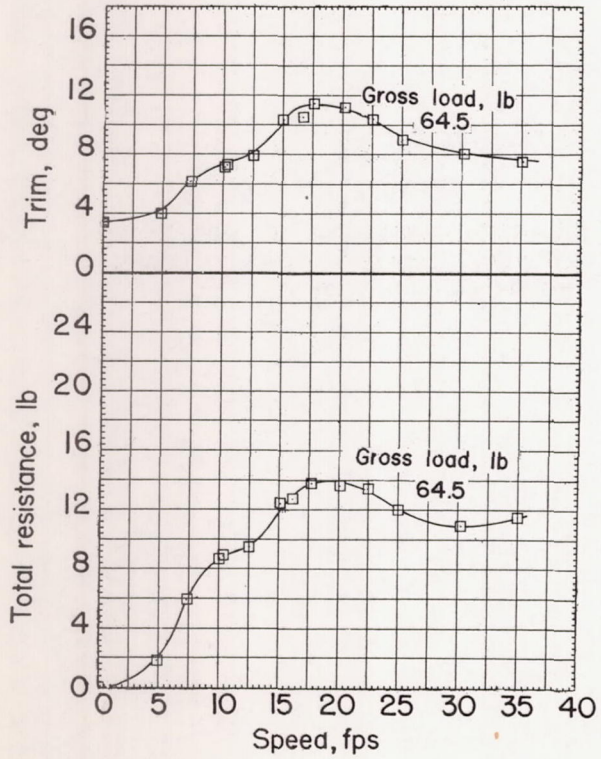


Figure 7.- Aerodynamic lift and pitching-moment coefficients. Center of moments, 24 percent M.A.C.; flap deflection, 20°; elevator deflection, -10°.



(a) Trim limits of stability with full power.

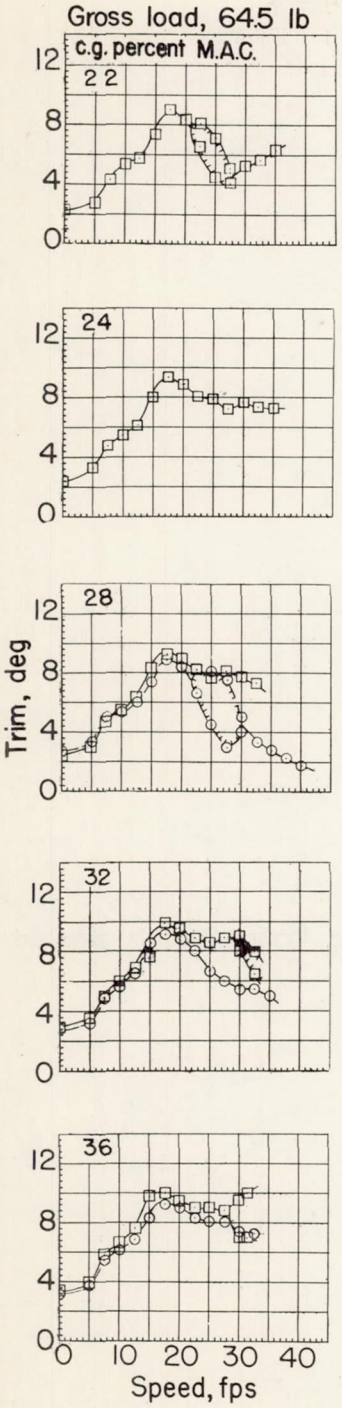


(b) Total resistance and trim without power.

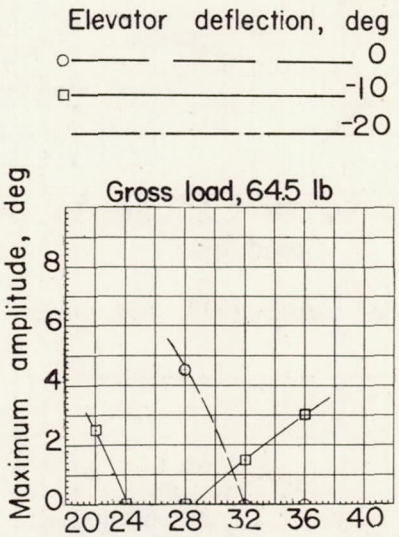
No landing records obtained.

(c) Variation of trim and draft during landing.

Figure 8.- Model 203A.

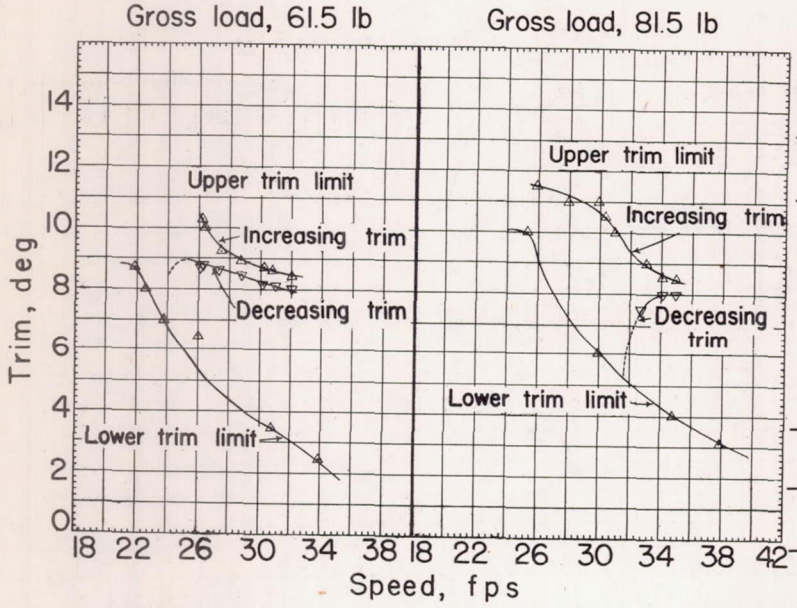


(d) Variation in trim with speed at full power.

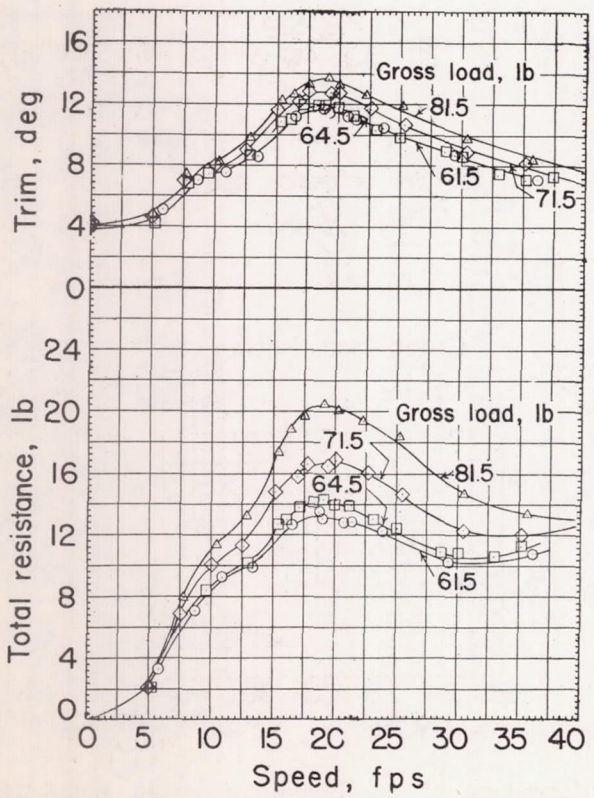


(e) Maximum amplitude of porpoising at different positions of the center of gravity at full power.

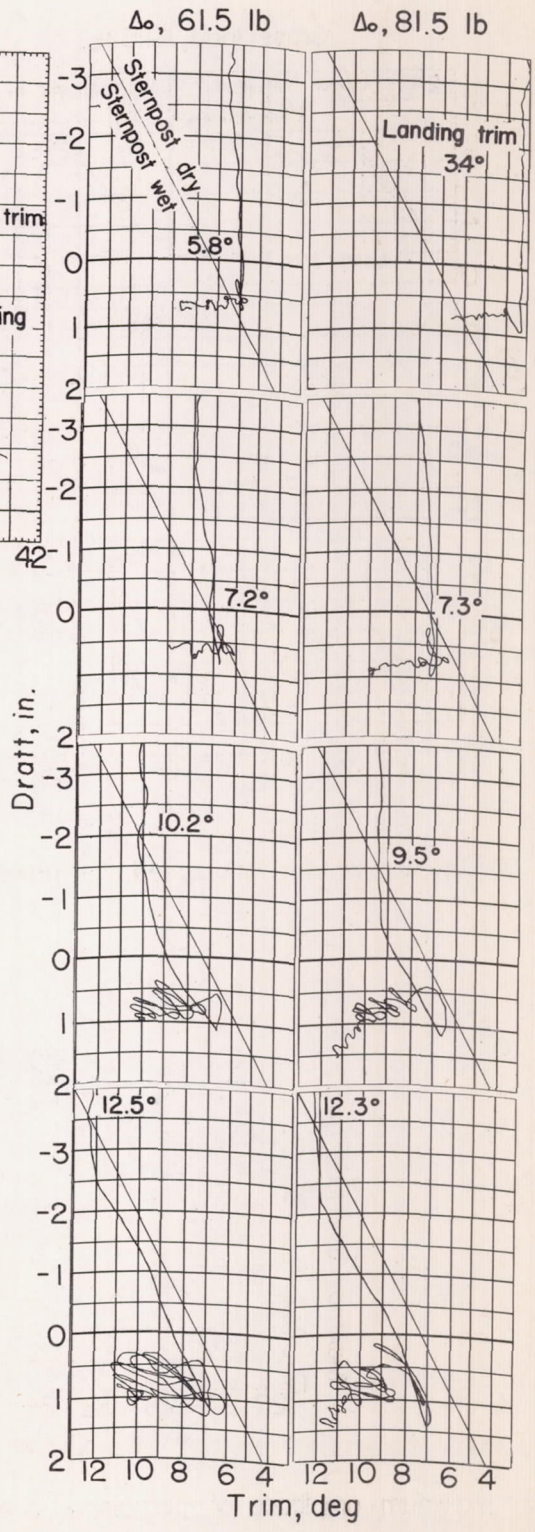
Figure 8.- Concluded.



(a) Trim limits of stability with full power.

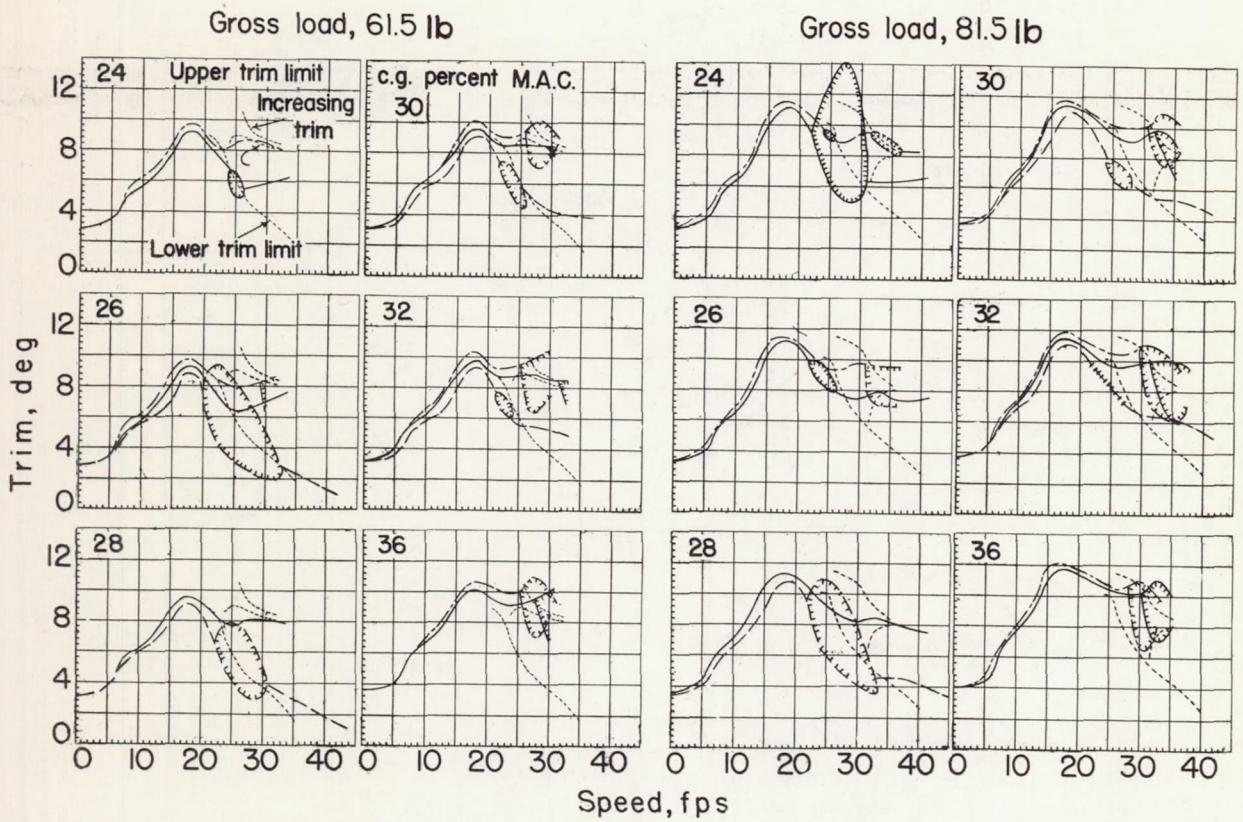


(b) Total resistance and trim without power.



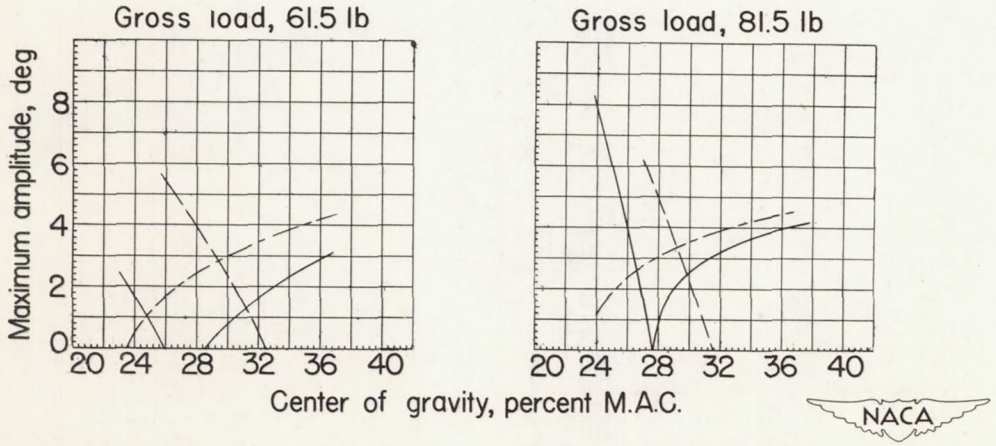
(c) Variation of trim and draft during landing.

Figure 9.- Model 203A-1.



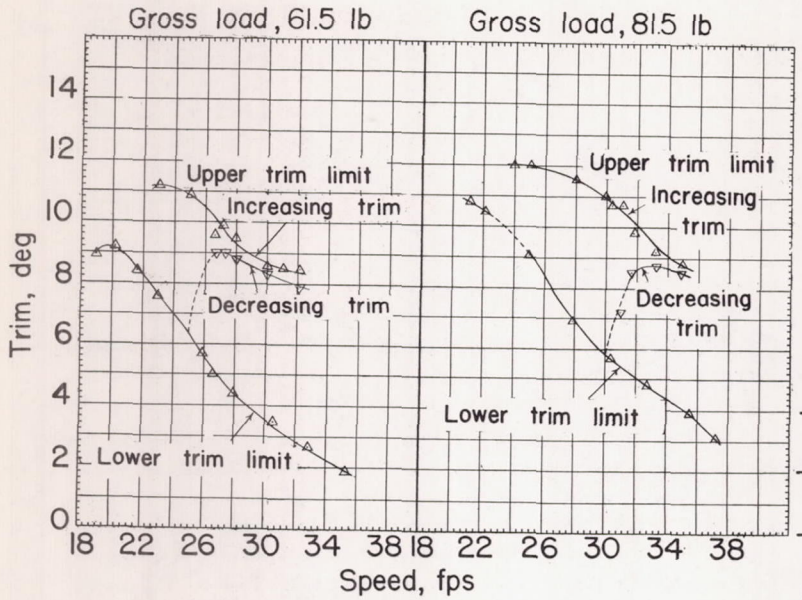
(d) Variation in trim with speed, full power.

Elevator deflection, deg
— — — 0
———— -10
—·—·— -20

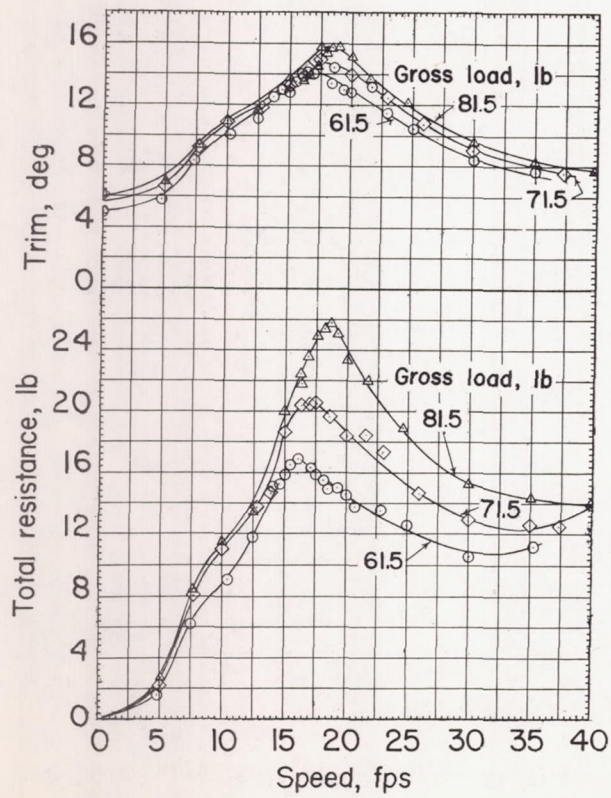


(e) Maximum amplitude of porpoising at different positions of the center of gravity, full power.

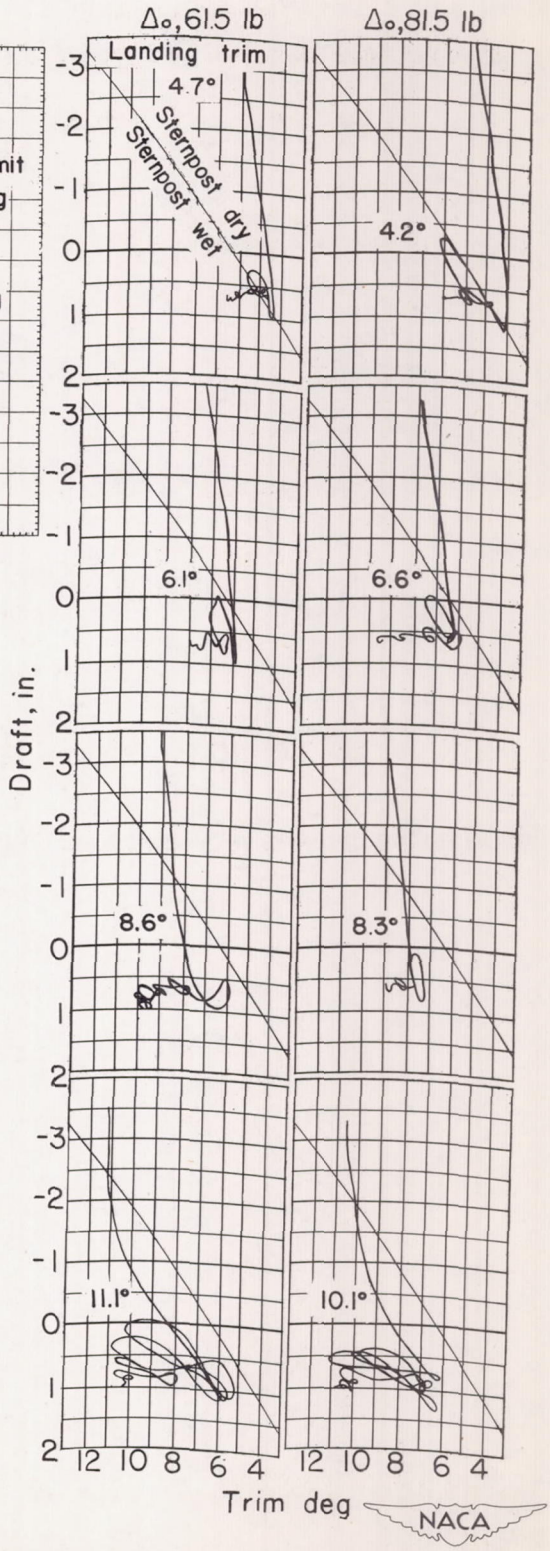
Figure 9.- Concluded.



(a) Trim limits of stability with full power.

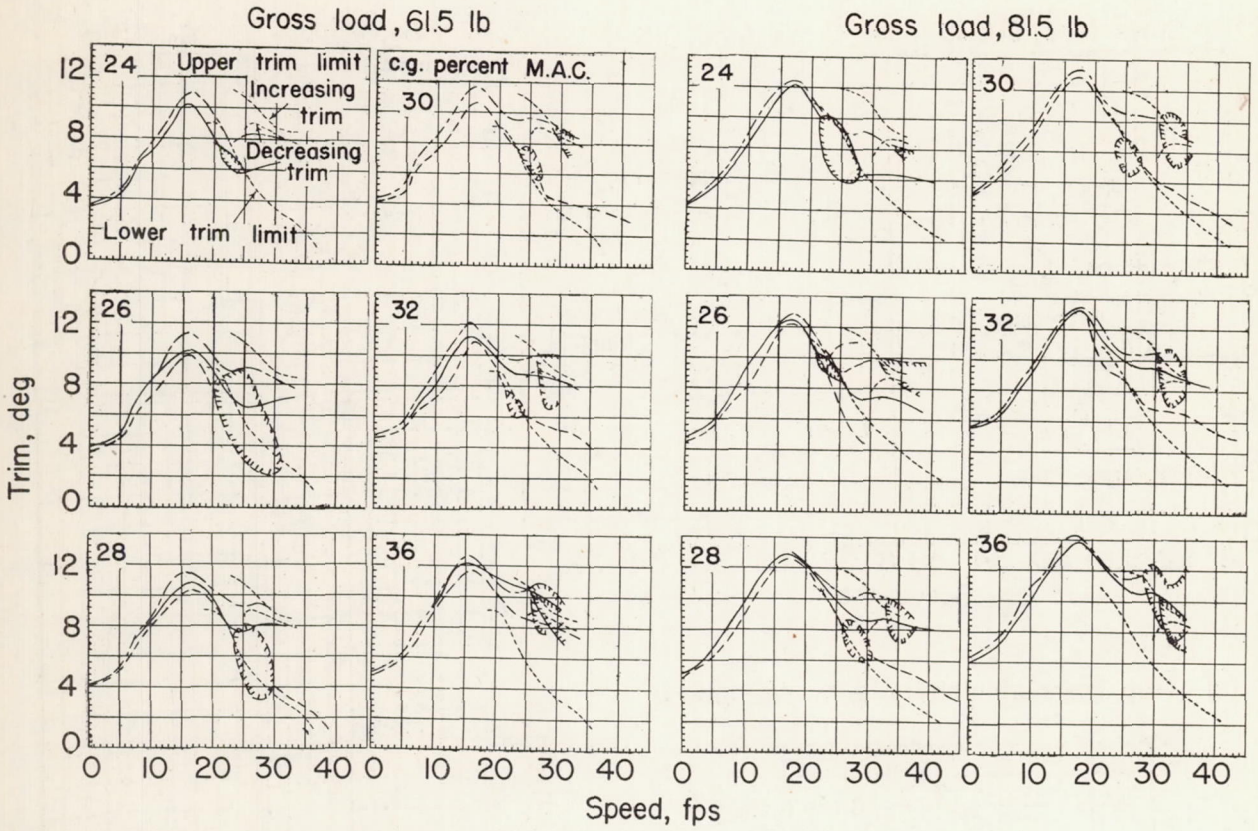


(b) Total resistance and trim without power.

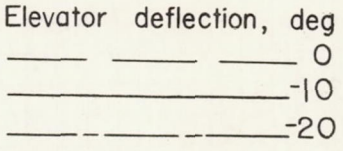


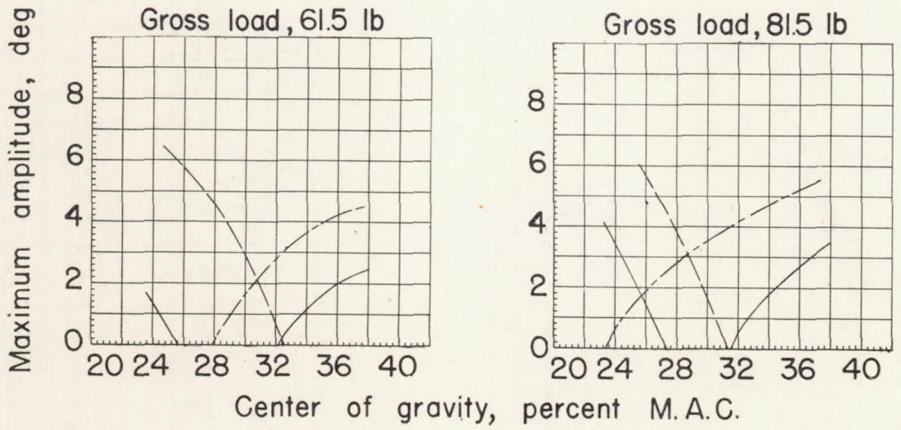
(c) Variation of trim and draft during landing.

Figure 10.- Model 203B.



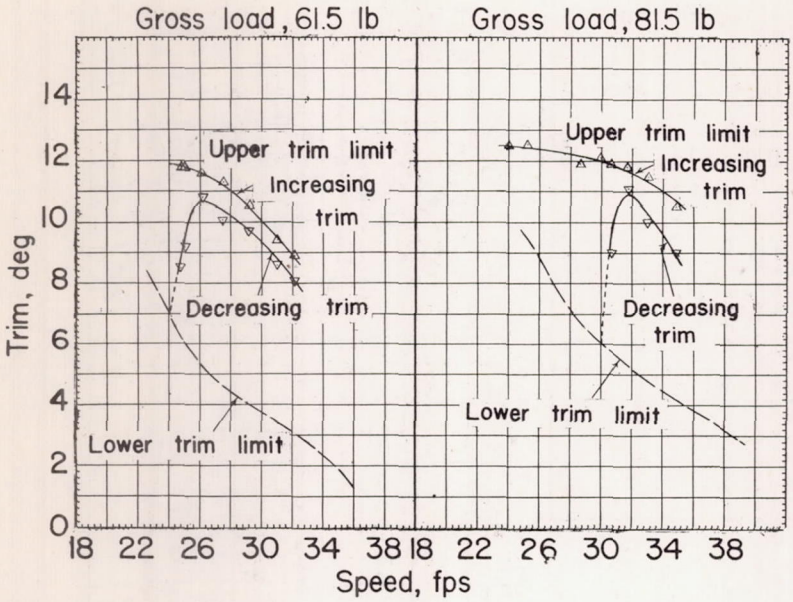
(d) Variation in trim with speed at full power.





(e) Maximum amplitude of porpoising at different positions of the center of gravity at full power.

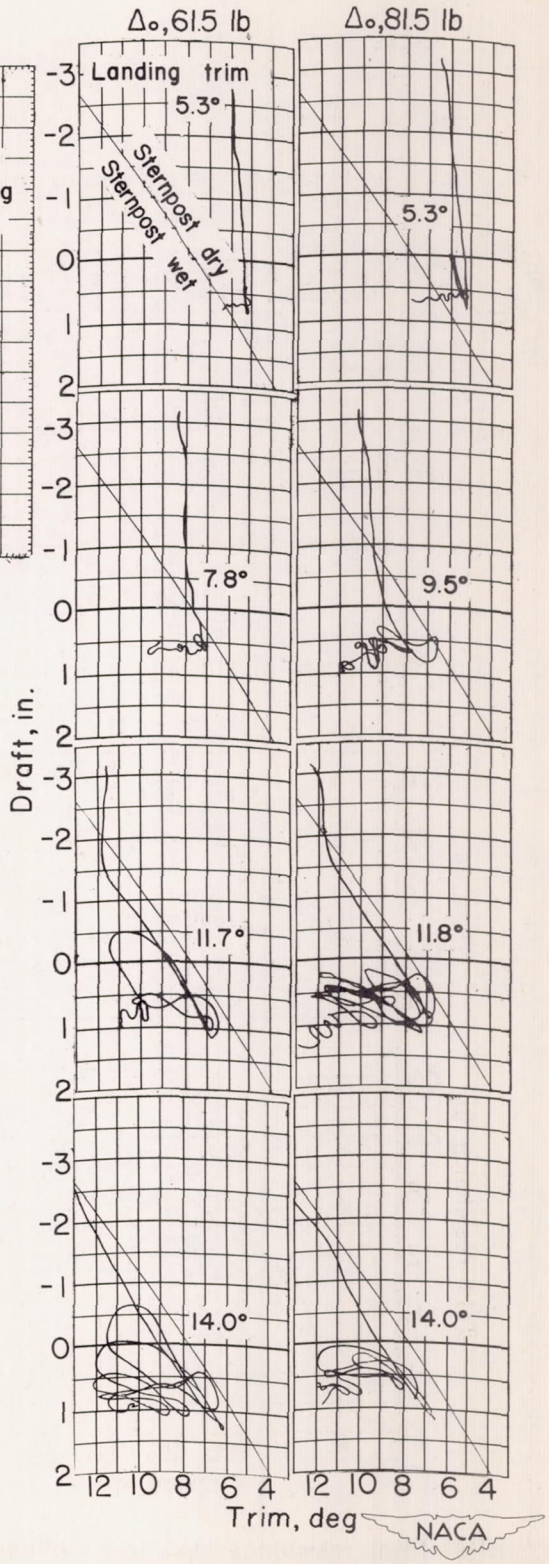
Figure 10.- Concluded.



(a) Trim limits of stability with full power.

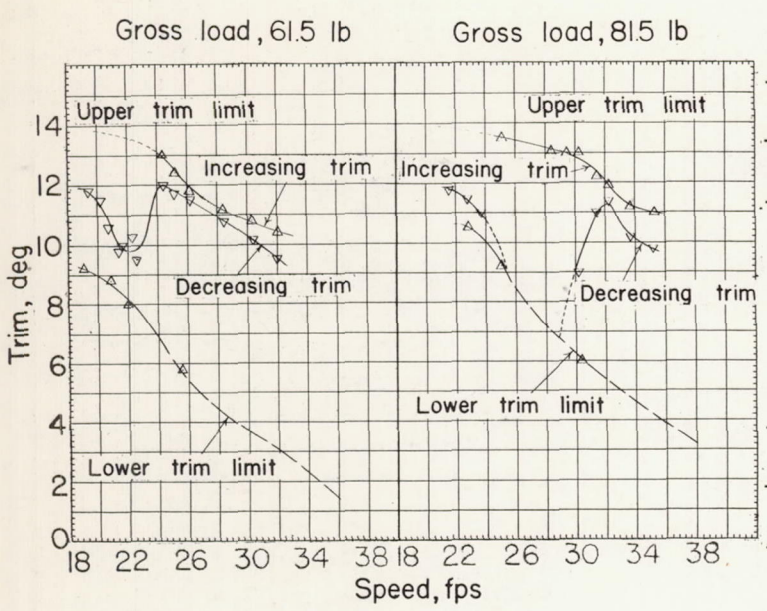
No resistance data obtained.

(b) Total resistance and trim without power.

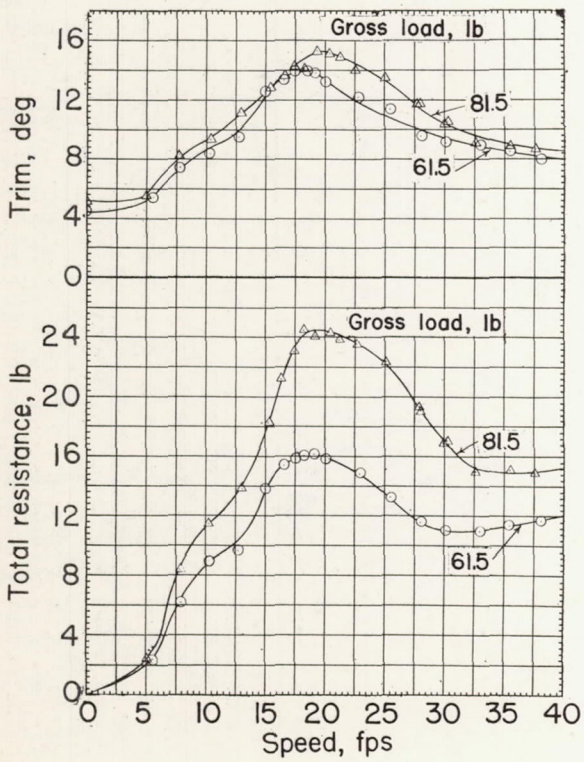


(c) Variation of trim and draft during landing.

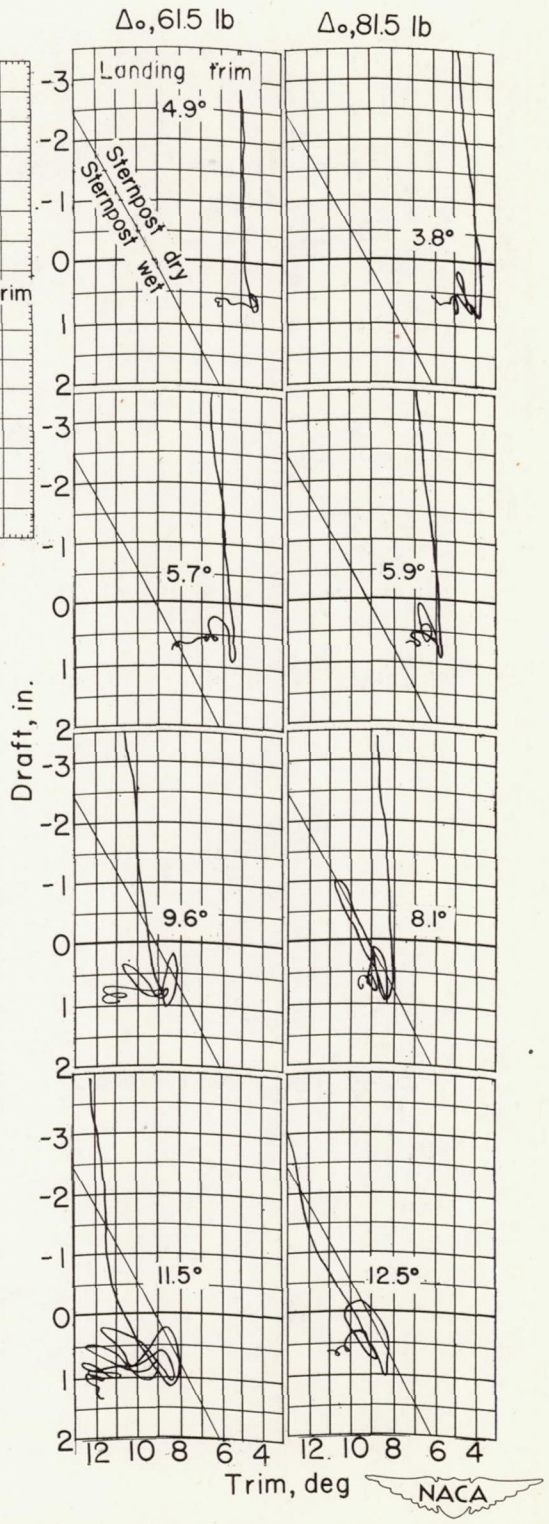
Figure 11.- Model 203B-1.



(a) Trim limits of stability with full power.

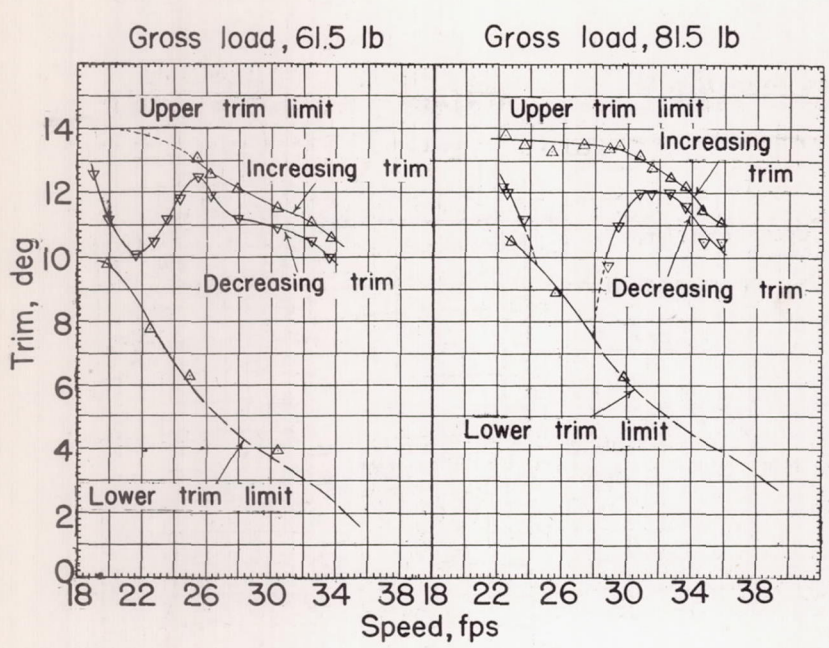


(b) Total resistance and trim without power.

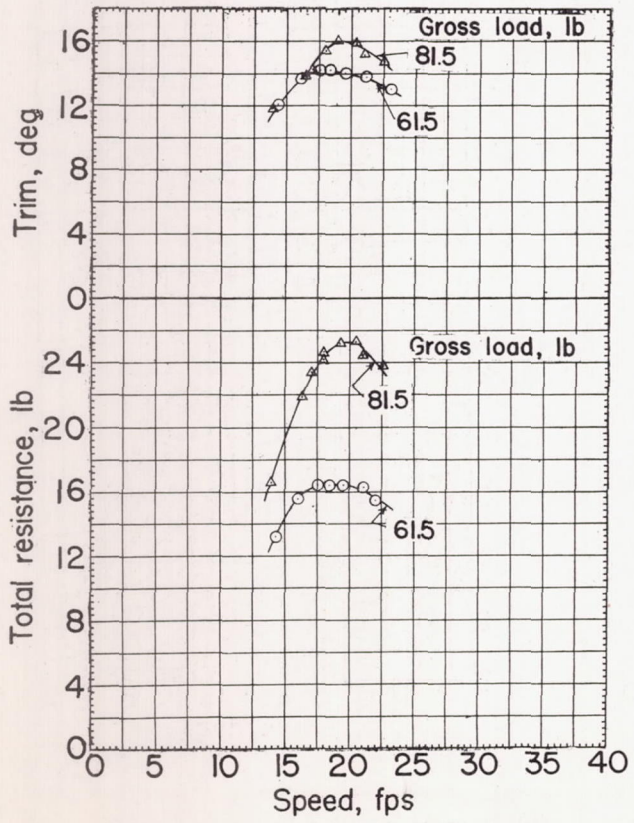


(c) Variation of trim and draft during landing.

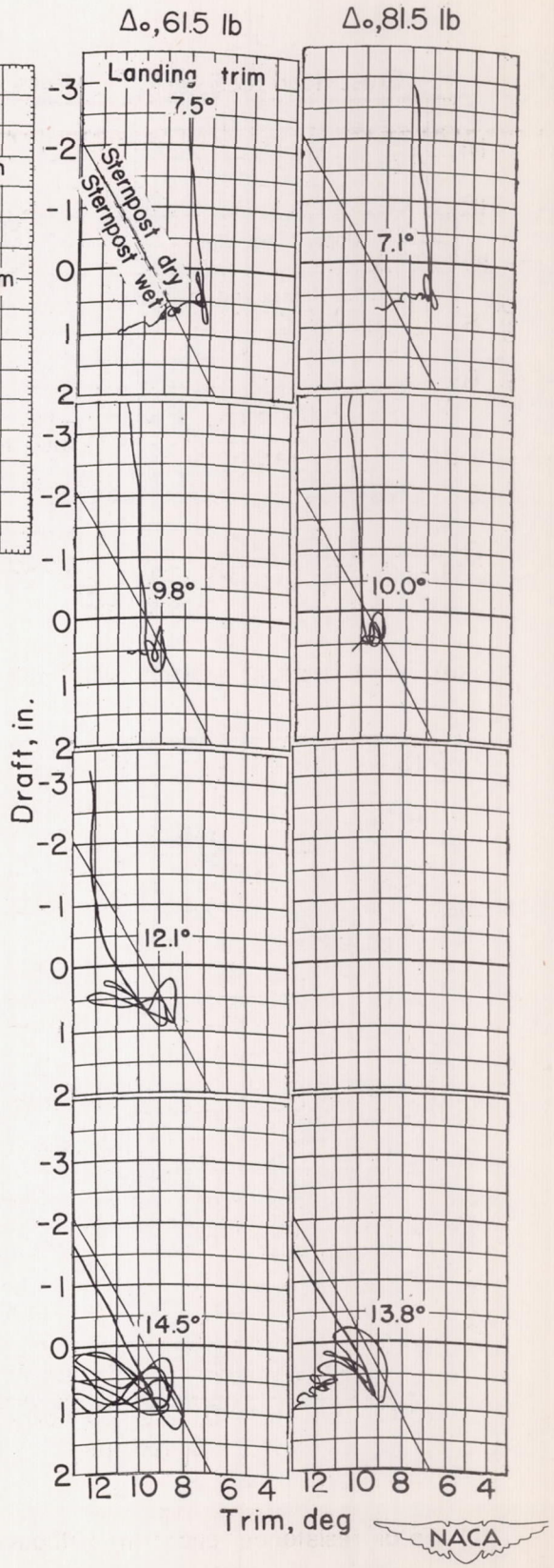
Figure 12.- Model 203A-1-a.



(a) Trim limits of stability with full power.

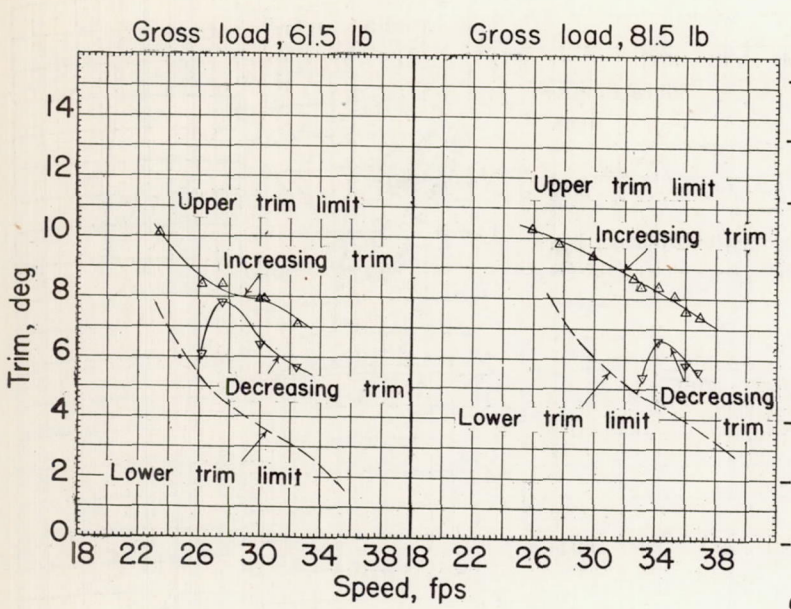


(b) Total resistance and trim without power.

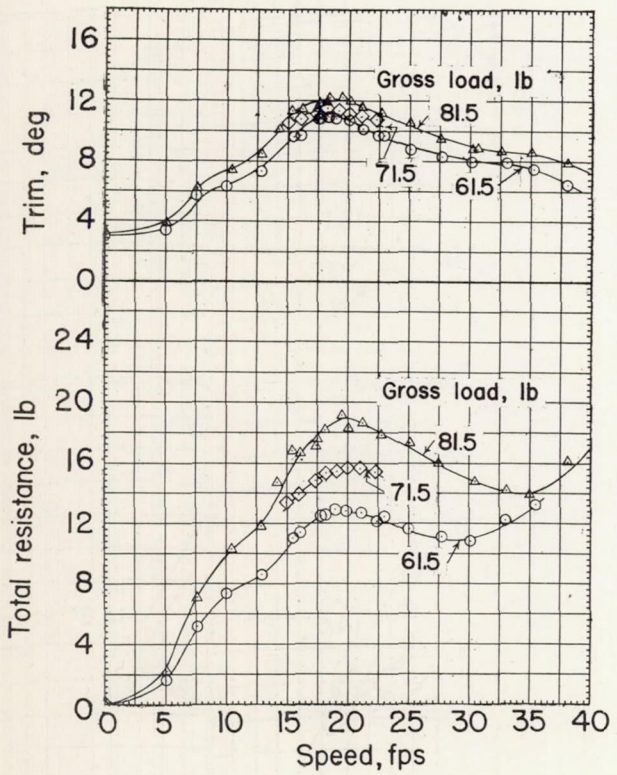


(c) Variation of trim and draft during landing.

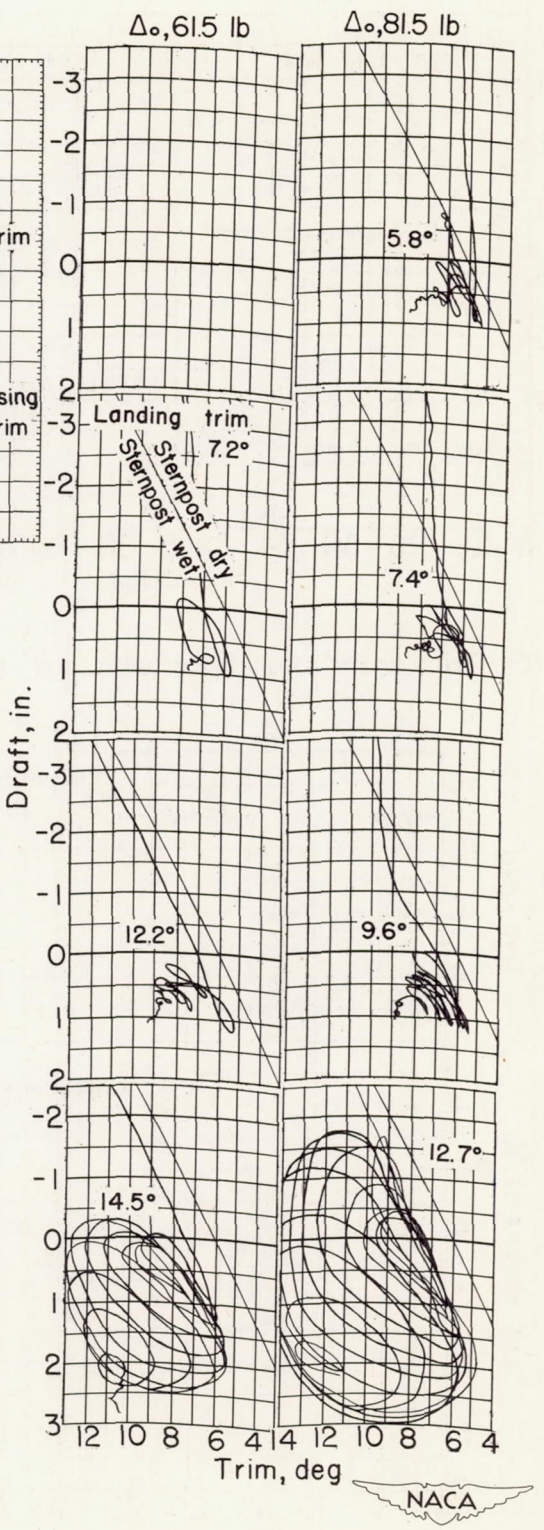
Figure 13.- Model 203A-2-a.



(a) Trim limits of stability with full power.

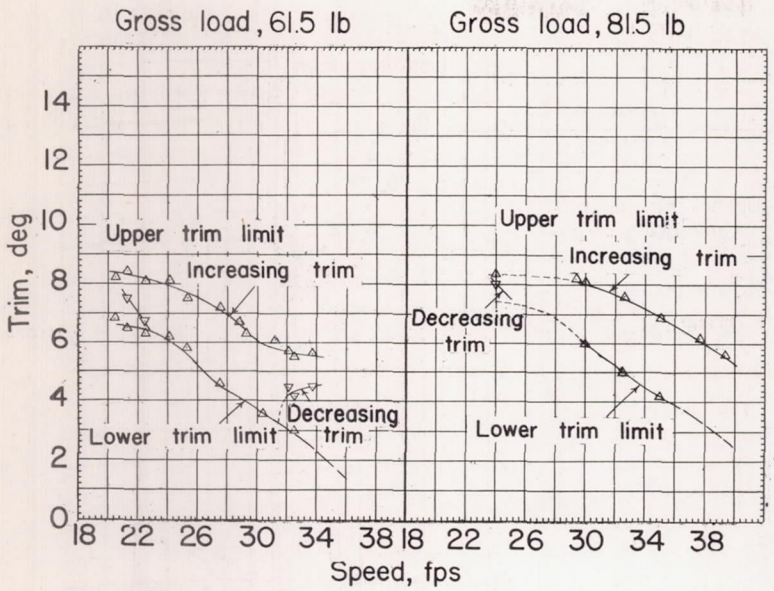


(b) Total resistance and trim without power.

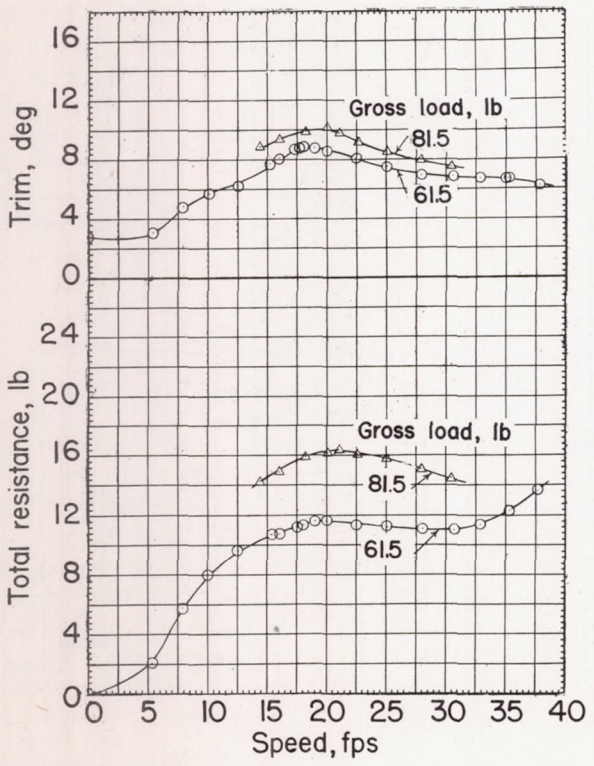


(c) Variation of trim and draft during landing.

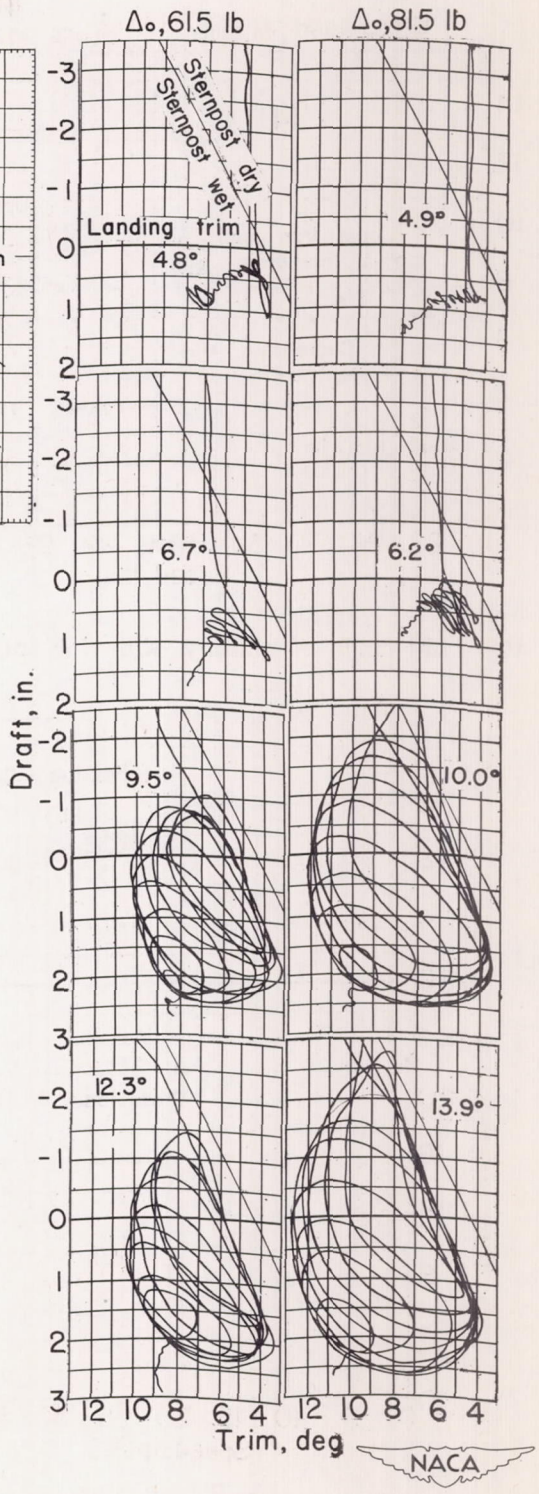
Figure 14.- Model 203A-3.



(a) Trim limits of stability with full power.

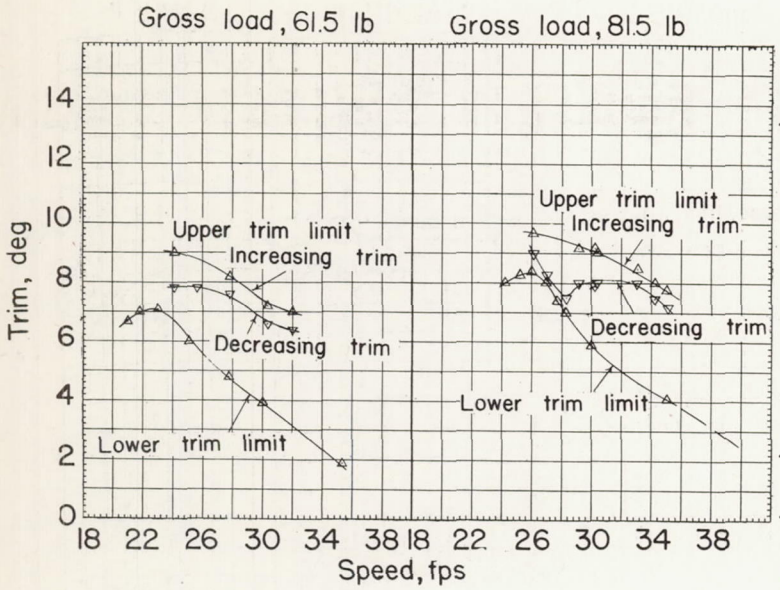


(b) Total resistance and trim without power.

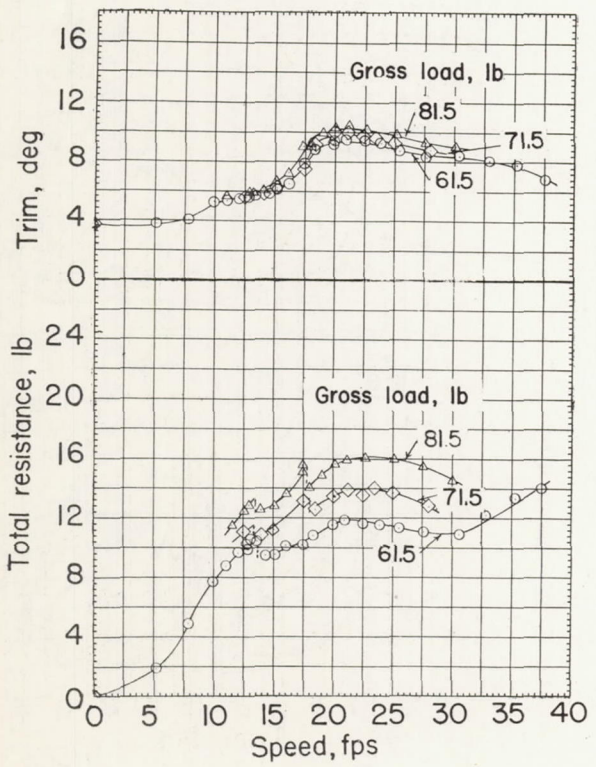


(c) Variation of trim and draft during landing.

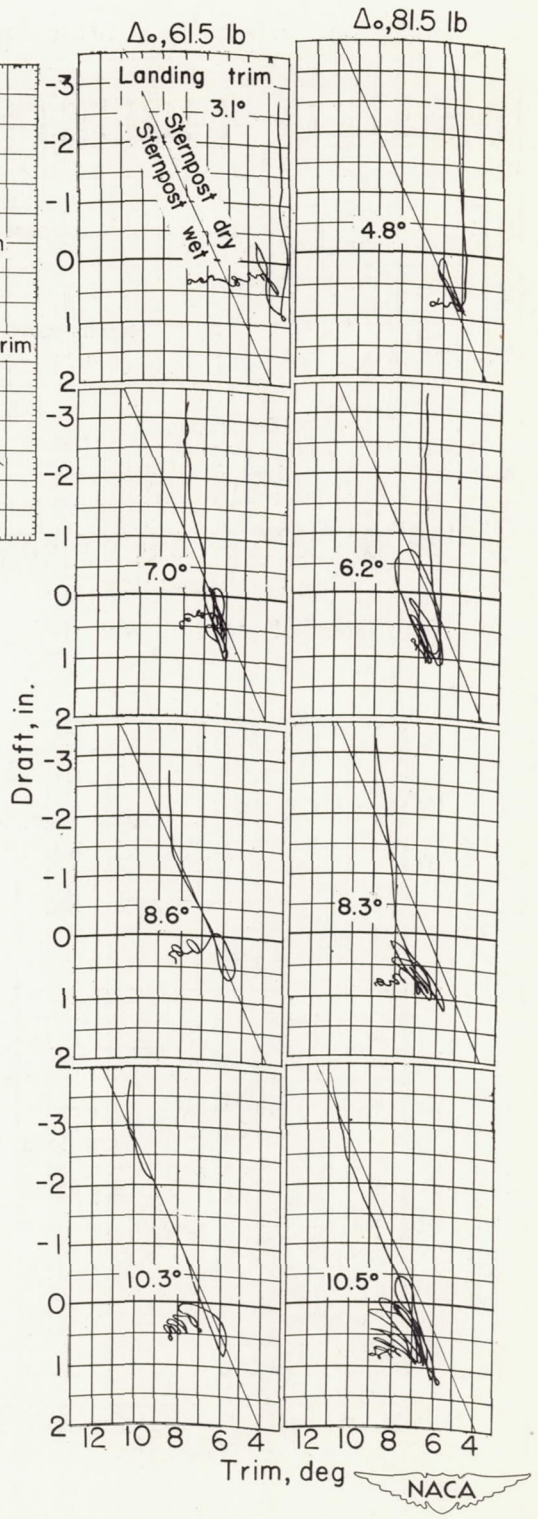
Figure 15.- Model 203A-b.



(a) Trim limits of stability with full power.

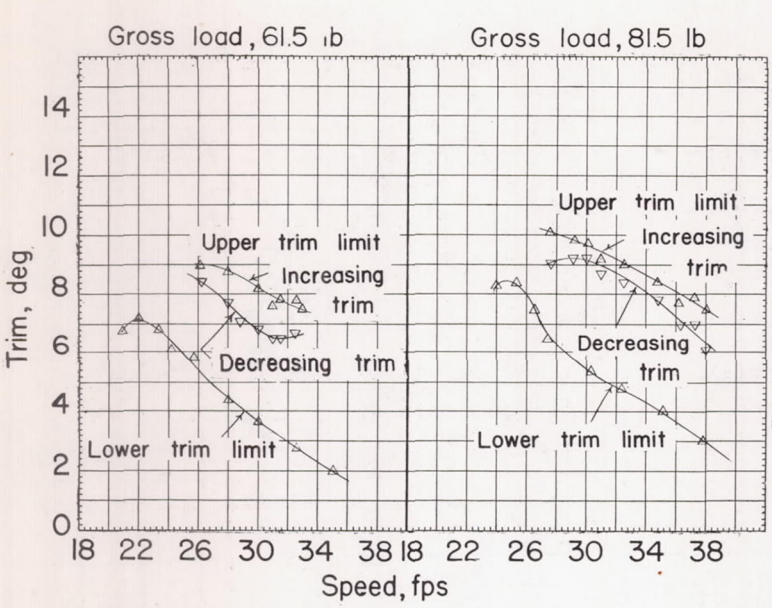


(b) Total resistance and trim without power.

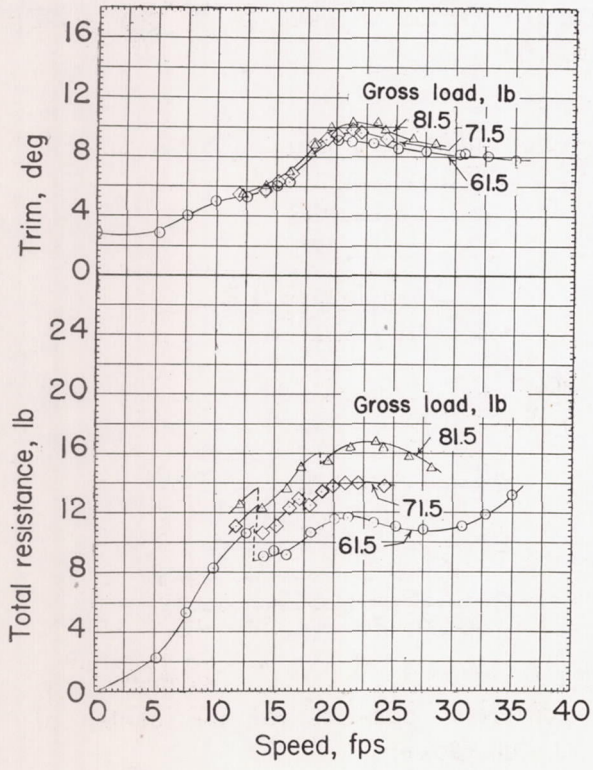


(c) Variation of trim and draft during landing.

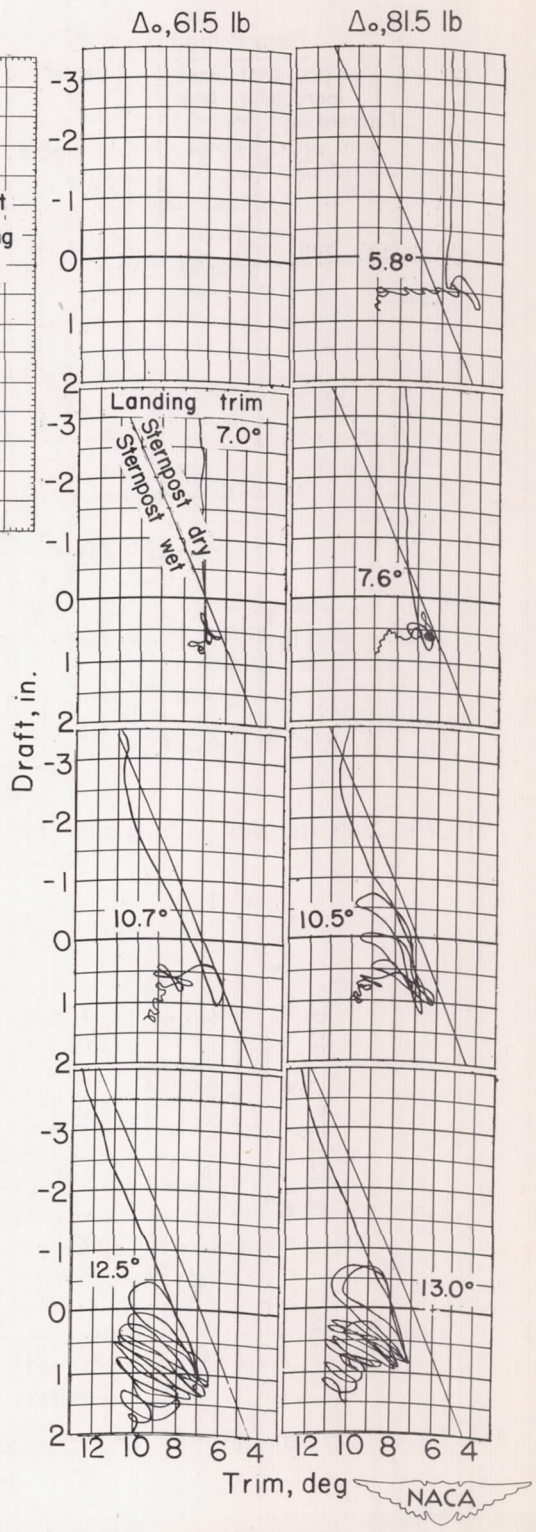
Figure 16.- Model 203C.



(a) Trim limits of stability with full power.

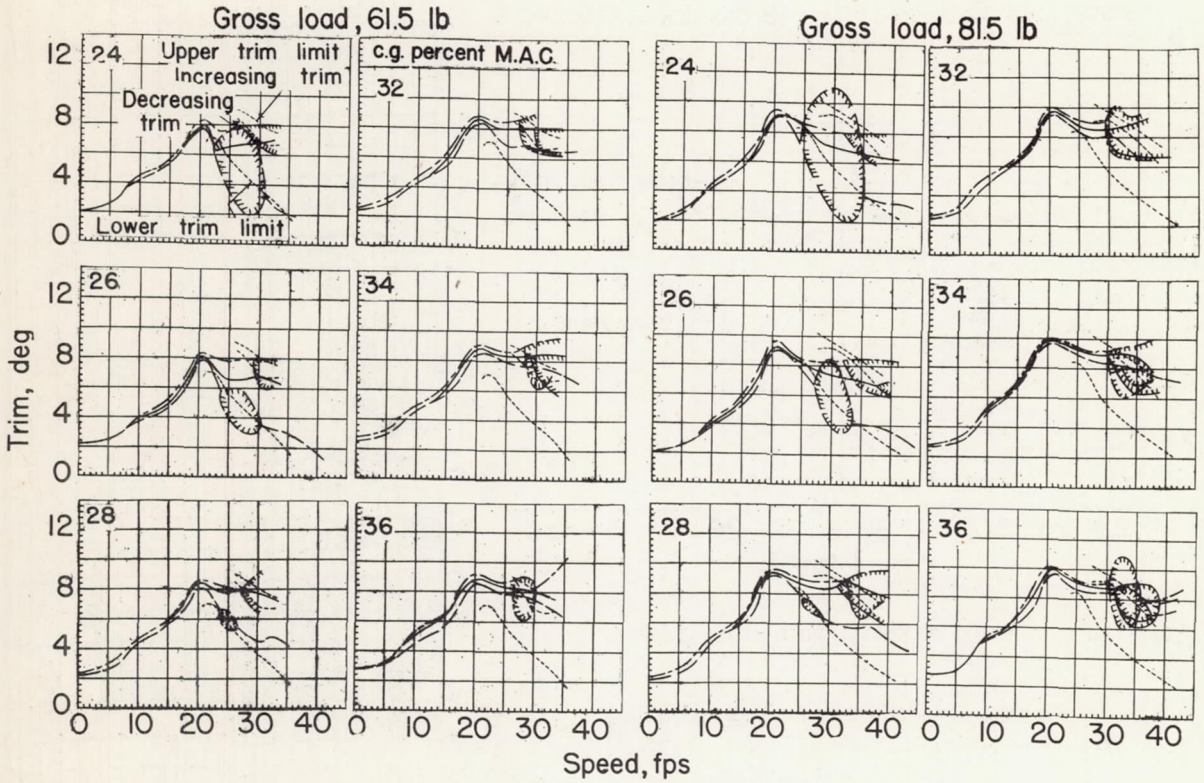


(b) Total resistance and trim without power.

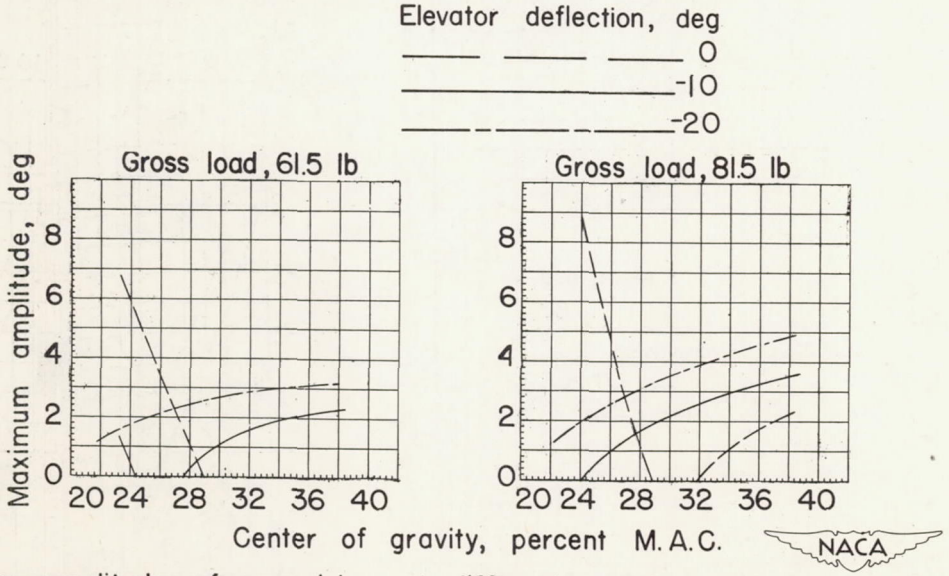


(c) Variation of trim and draft during landing.

Figure 17.- Model 203C-1.



(d) Variation in trim with speed at full power.



(e) Maximum amplitude of porpoising at different positions of the center of gravity at full power.

Figure 17.- Concluded.

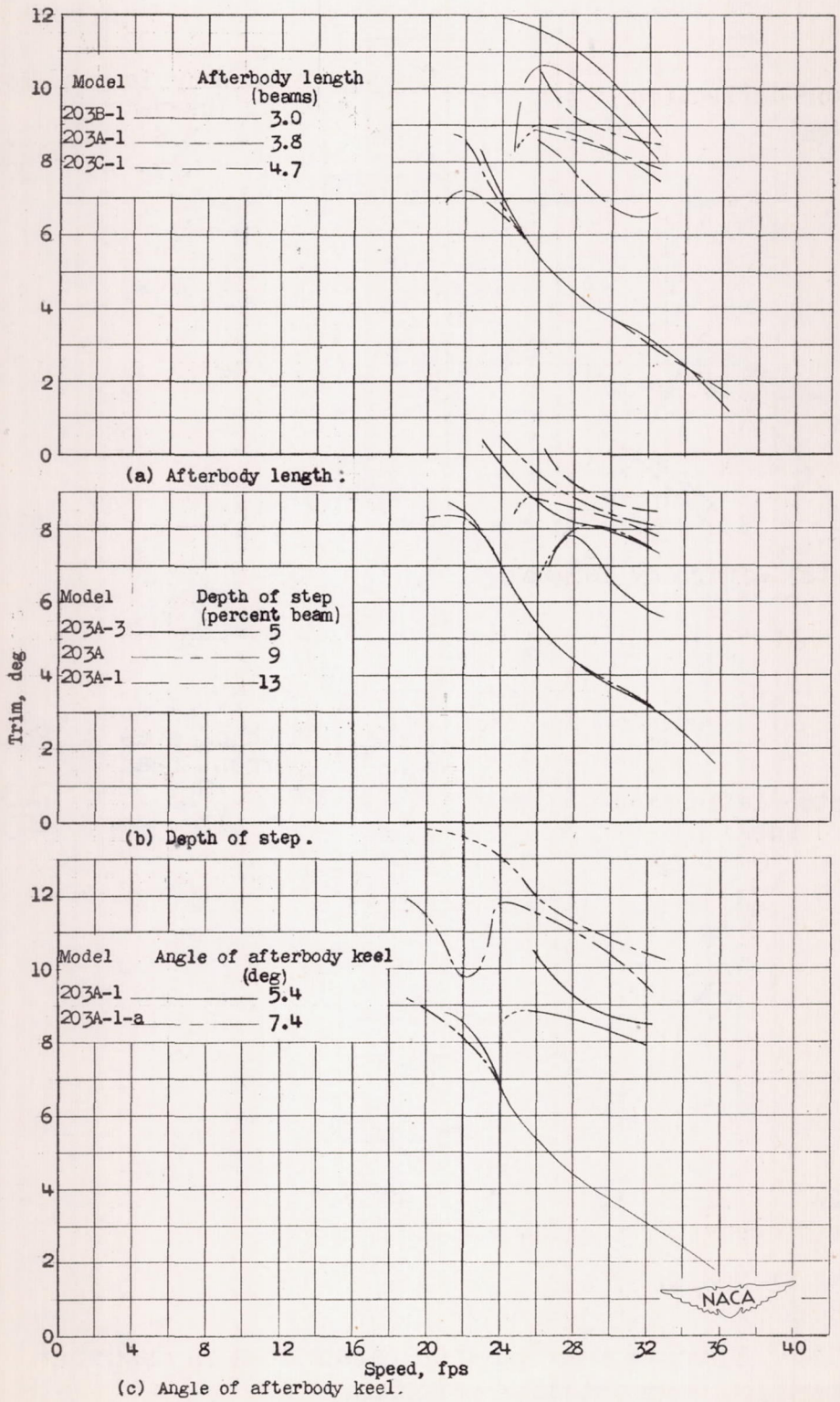
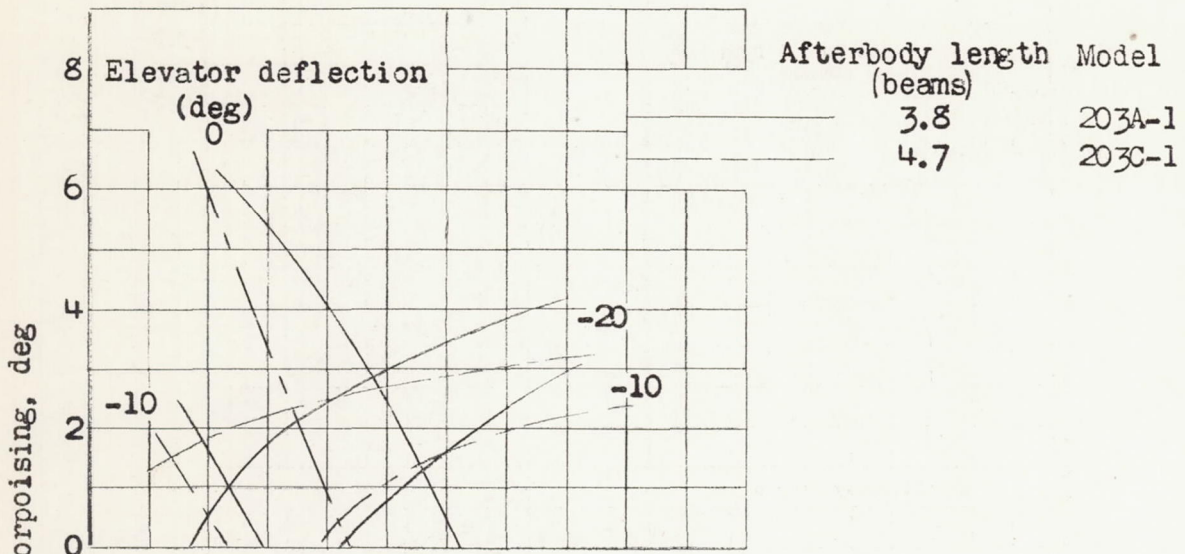
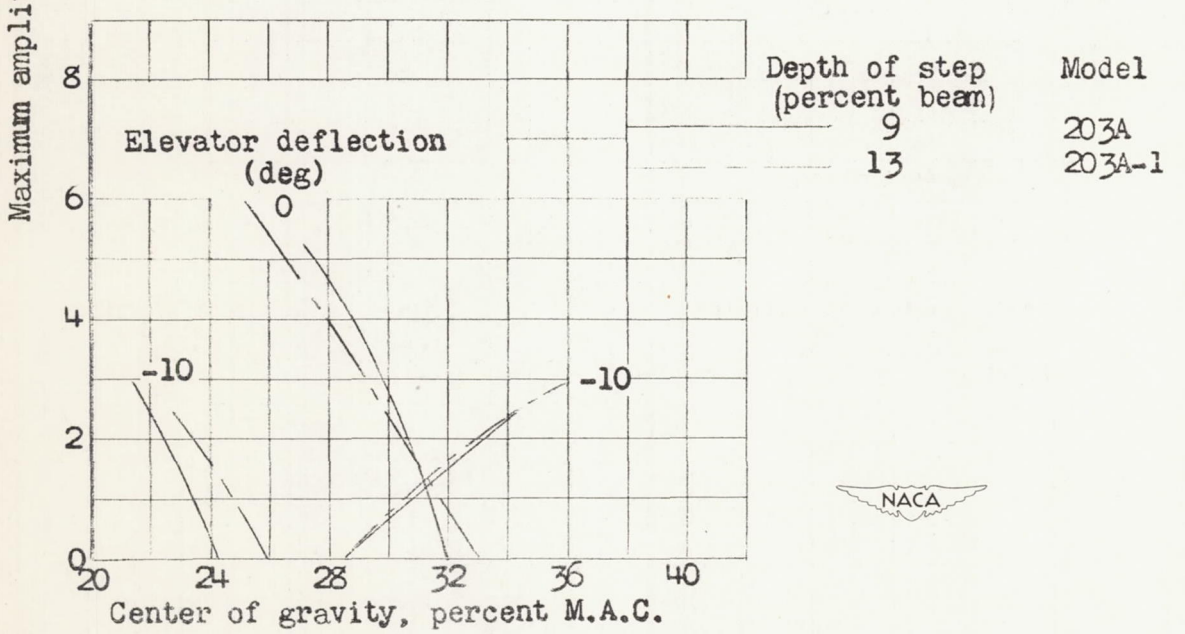


Figure 18.- Effect of afterbody hull parameters on trim limits of stability.



(a) Afterbody length.



(b) Depth of step.

Figure 19.- Effect of afterbody hull parameters on maximum amplitude of porpoising.

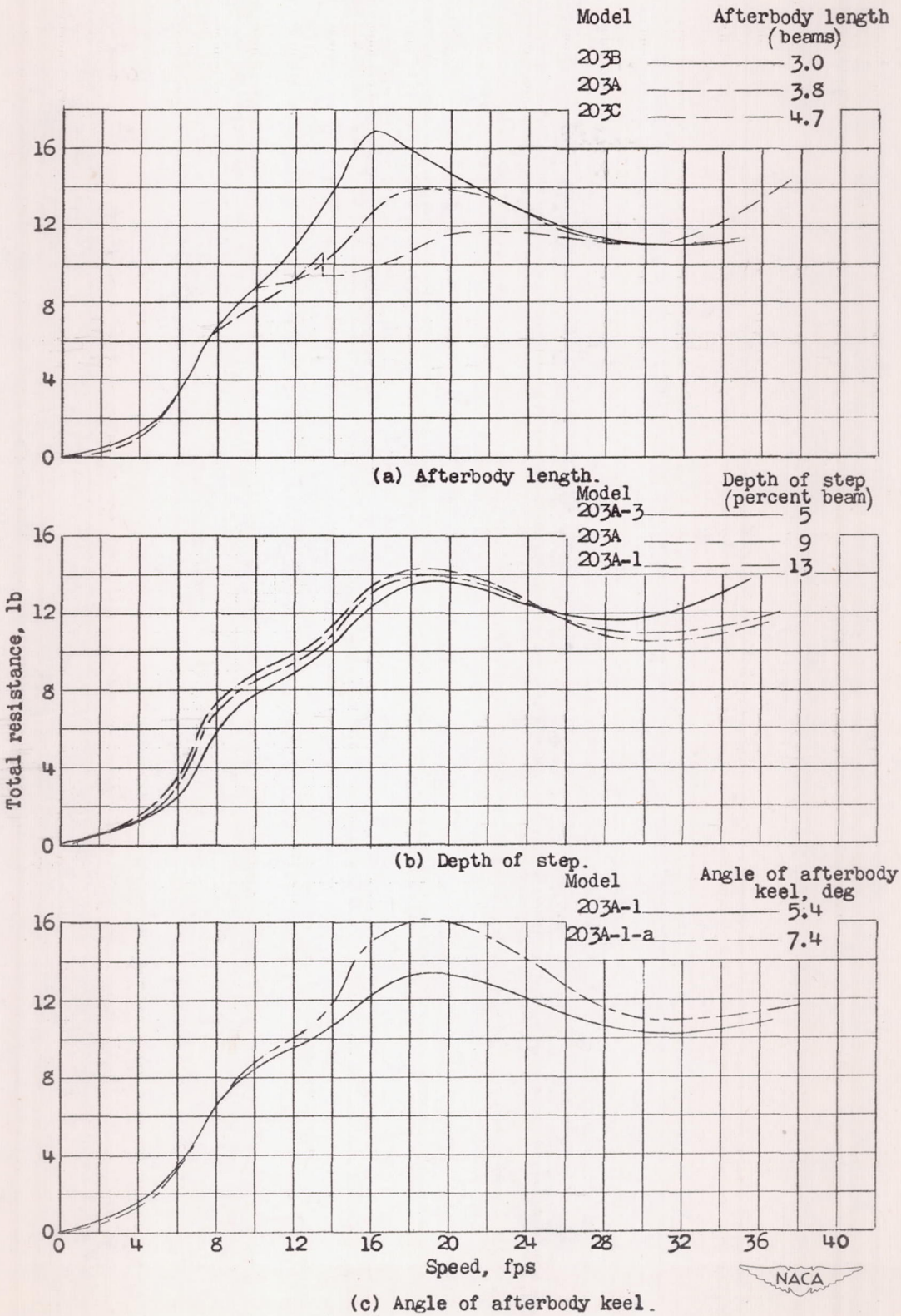


Figure 20.- Effect of afterbody hull parameters on total resistance.

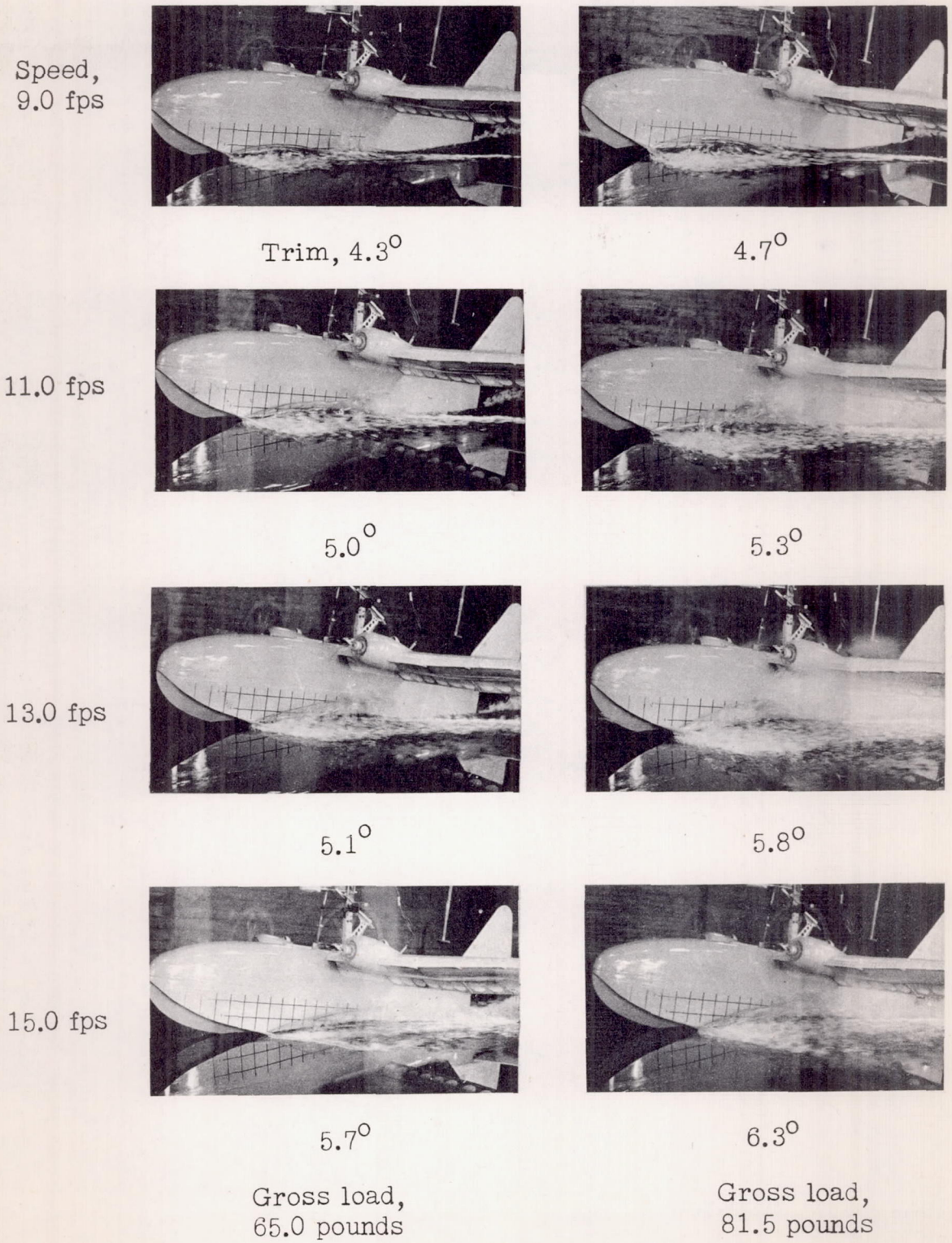


Figure 21.- Bow spray characteristics with full power of model 203C-1.

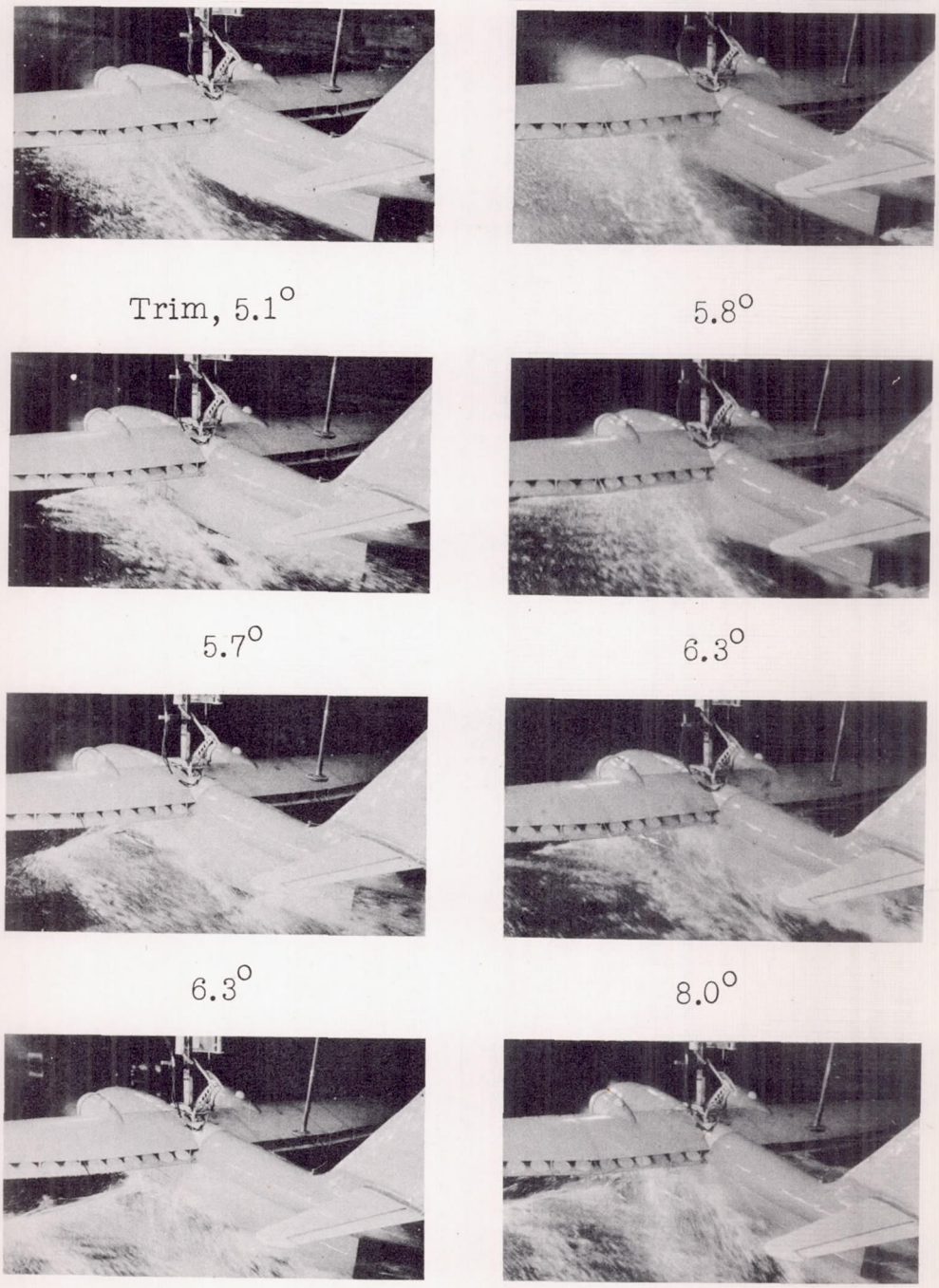


Figure 22.- Stern spray characteristics with full power of model 203C-1.

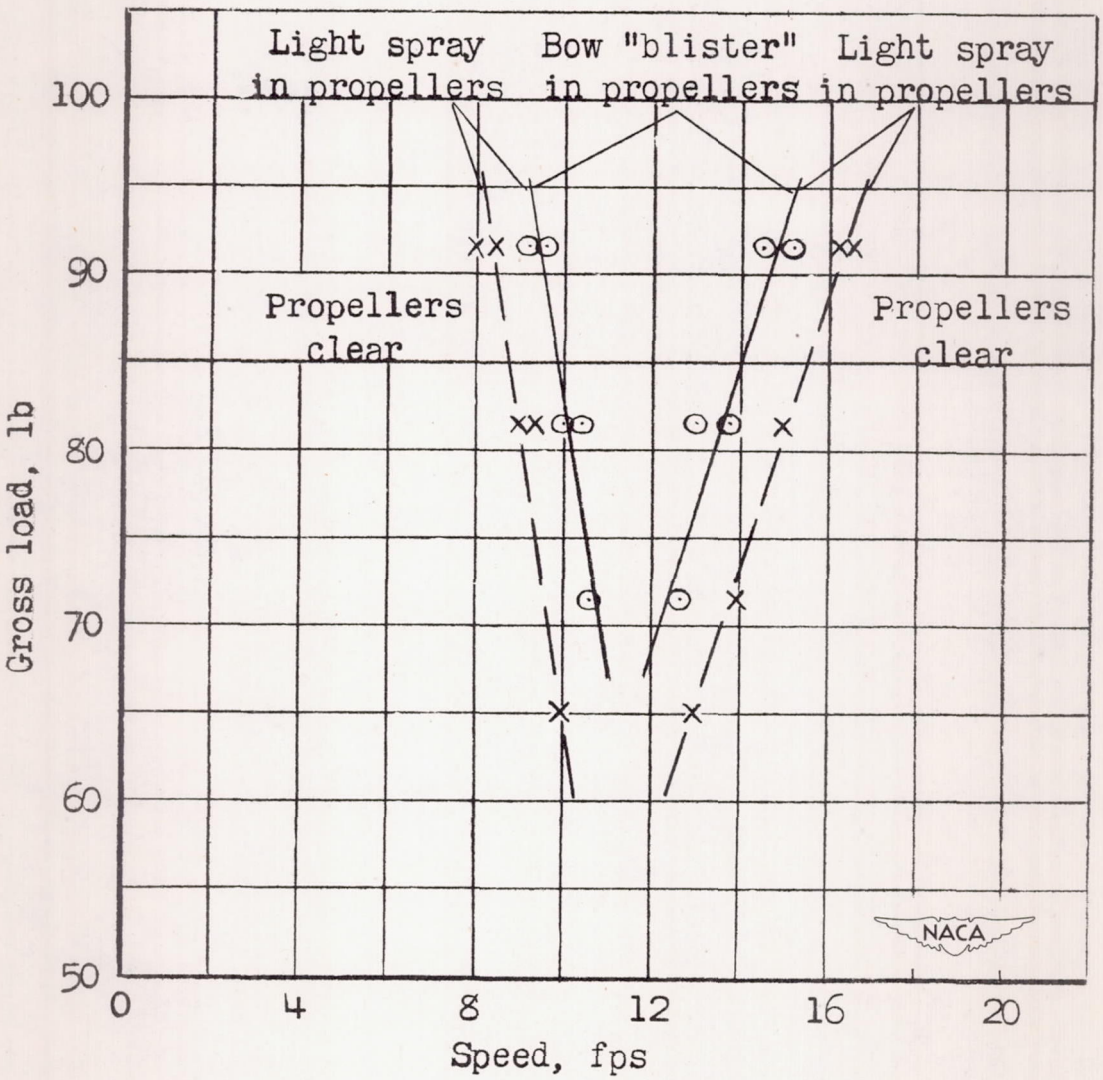


Figure 23.- Speed range over which spray enters the propellers of model 203C-1.